THESIS FOR THE DEGREE OF DOCTOR OF PHILOSOPHY

Advances in Soft Matter Nanofabrication

MEHRNAZ SHAALI

Department of Chemistry and Chemical Engineering
CHALMERS UNIVERSITY OF TECHNOLOGY
Gothenburg, Sweden 2015

Advances in Soft Matter Nanofabrication

MEHRNAZ SHAALI

ISBN: 978-91-7597-237-4

Doktorsavhandlingar vid Chalmers tekniska högskola

Serie Nr 3018

ISSN 0346-718X

Department of Chemistry and Chemical Engineering

Chalmers University of Technology

SE-412 96 Gothenburg

Sweden

Telephone + 46 (0)31-772 1000

Front Cover:

[Artist's representation of confined lipid monolayers on nanopatterned Teflon AF surface]

Printed by Chalmers Reproservice

Gothenburg, Sweden 2015

تقدیم به فرهیختهٔ آموزگاران زندگی ام هما و جعفر

To my parents, Homa and Jafar

ADVANCES IN SOFT MATTER NANOFABRICATION

Mehrnaz Shaali
Department of Chemistry and Chemical Engineering
Chalmers University of Technology

ABSTRACT

The focus of this thesis is placed on the fabrication of engineered nanodevices for the manipulation of soft matter thin films. By combining top-down micro- and nanofabrication approaches with bottom-up self-assembly strategies, new research platforms were developed, tested and characterized.

A large part of the studies described herein were performed on electron beam-sculpted Teflon AF surfaces, which served as substrate for molecular lipid films and biological cells. The effects of e-beam exposure of Teflon AF deposits, including changes in hydrophobicity, topography, surface potential and roughness, have been investigated in detail. Lipophilic nanolanes of 50 nm width were created in this manner. The studies show, for example, how spreading of a phospholipid monolayer film originating from a single giant multilamellar vesicle source can be confined and guided by e-beam-exposed frames on the polymer surface. The studies also reveal the preferential adhesion of biological cells on these e-beam-treated Teflon AF surfaces, where the shape of the patterned areas strongly affects cell adhesion.

By applying perfluorinated solvent as developer to complete the ebeam-lithography procedure, Teflon AF was introduced as non-amplified negative e-beam resist. Nanostructures with feature sizes as small as 30 nm in width and 40 nm in pitch were fabricated. This new resist was characterized by determining its contrast, sensitivity, and film thickness. The accommodation of single DNA origami scaffolds on developed Teflon AF nanopillars has been investigated as an exemplary application, and about 80% coverage of the available pillar surface was achieved.

Moreover, a novel, contact-free technology was developed to generate surface-supported networks of lipid nanotubes and flat giant unilamellar vesicles on a micro-patterned SU-8 substrate. The nanotubes were formed by thermomigration of a phospholipid double bilayer, where the migration of lipid material on the patterned surface was initiated and controlled by a temperature gradient created with an IR laser.

In the work presented here, a number of specific problems have been tackled in an interdisciplinary approach, making use of micro- and nanotechnologies, new materials and biomimetic principles that can open up new experimental opportunities to address further fundamental research questions.

Keywords: Phospholipid, monolayer, double bilayer, Teflon AF, lipid nanotube, electron beam lithography, photolithography, confocal microscopy, AFM, KPFM, DNA origami, cells, negative e-beam resist

LIST OF PUBLICATIONS

This thesis is based on the work presented in the following papers:

I. Nanopatterning of Mobile Lipid Monolayers on Electron-Beam-Sculpted Teflon AF Surfaces

Mehrnaz Shaali, Samuel Lara Avila, Paul Dommersnes, Alar Ainla, Sergey Kubatkin and Aldo Jesorka
ACS Nano, **2015,** DOI: 10.1021/nn5050867

II. Cell Patterning on Electron Beam Exposed Teflon AF Surfaces

Mehrnaz Shaali, Kent Jardemark, Samuel Lara-Avila, Sergey Kubatkin, and Aldo Jesorka
Submitted

III. DNA Nanopatterning on Teflon Amorphous Fluoropolymer: Introducing a New Non-Amplified Negative E-Beam Resist

Mehrnaz Shaali, Jakob G. Woller, Jonas K. Hannestad, Patrik G. Johansson, Nesrine Aissaoui, Laura De Battice, Tom Brown, Afaf H. El-Sagheer, Sergey Kubatkin, Samuel Lara-Avila, Bo Albinsson, and Aldo Jesorka
Submitted

IV. Thermal Migration of Molecular Lipid Films as a Contactless Fabrication Strategy for Lipid Nanotube Networks

Irep Gözen, Mehrnaz Shaali, Alar Ainla, Bahanur Ortmen, Inga Põldsalu, Kiryl Kustanovich, Gavin D. M. Jeffries, Zoran Konkoli, Paul Dommersnesc and Aldo Jesorka
Lab-on-a-Chip, **2013**, DOI: 10.1039/c3lc50391g

CONTRIBUTION REPORT

Paper I. Designed and performed all the experiments, analyzed the data and wrote the paper.

Paper II. Designed and performed all the experiments, analyzed the data and wrote the paper.

Paper III. Contributed to the design and perform of the experiment. Fabricated and characterized the surfaces. The main author of the paper.

Paper IV. Fabricated the patterned SU8 surfaces and performed the characterization analysis of the surfaces.

RELATED PATENT APPLICATIONS

Lithographic pattern development process for amorphous fluoropolymer

Aldo Jesorka & Mehrnaz Shaali

US20140065551 A1, Priority: Sep 6th, 2012.

LIST OF ABBREVIATIONS

AFM	Atomic Force Microscopy
BSE	Back scattered electrons
CHO	Chinese hamster ovary
CPD	Contact potential difference
CPP	Critical packing parameter
DIC	Diffraction interference contrast
DMEM	Dulbecco's modified eagle medium
EBL	Electron beam lithography
FBS	Fetal bovin serum
FFV	Free fractional volume
FGUV	Flat giant unilamellar vesicle
FIB	Focused ion beam
HEK	Human embryonic kidney
HSQ	Hydrogen silsesquioxane
KPFM	Kelvin probe force microscopy
LIFM	Laser-induced fluorescence microscopy
MEM	Modified Eagle's medium
MLV	Multilamellar vesicle
NA	Numerical aperture
PA	Phosphatidic acid
PC	Phosphatidylcholine
PDD	2, 2-bis-trifluoromethyl-4, 5-difluoro-1, 3-dioxole
PE	Phosphatidylethanolamine
PE	primary electrons
SE	Secondary electrons
SEM	Scanning electron microscopy
SPM	scanning probe microscopy
SR	Synchrotron radiation
STORM	Stochastic optical reconstruction microscopy
TAF	Teflon AF
T_g	Glass transition temperature
TIRF	Total internal reflection microscopy
WCA	Water contact angle
XPS	X-ray photoelectron spectroscopy

CONTENTS

1. INTRODUCTION

It's not possible to talk about nanoscience without mentioning the name of Richard P. Feynman, the Nobel prize laureate in physics, who in his famous talk in 1959 focused the world's attention to the possibilities of "manipulating and controlling things on a small scale".[1] Even though he didn't use the term "nanotechnology", many of the possibilities that he outlined, such as manipulating individual atoms, fabricating very small devices, or miniaturizing computer components to reach the atomic scale, are nowadays established research fields.

However, nanotechnology, i.e., "the study and control of phenomena and materials at length scales below 100 nm",[2] as we know it today, had to wait about two decades until the invention of the scanning tunneling microscope by Binning and Rohrer. With this instrument, "seeing" nanostructures at the atomic level became possible.[3-4] Since then, a massive research and commercialization effort has been made towards exploring and utilizing the nano world.

As an inevitably interdisciplinary field, involving physics, chemistry, biology and other branches of science, nanoscience and technology builds upon the fact that many of the physical effects that are negligible on macroscopic scales become dominant when decreasing the dimensions of the system (Scaling laws).[5-6] Thereby a new set of quite different properties of the materials exists in nanosystems that cannot be observed on the macro and micro scale. The more prominent role of quantum effects at nano dimensions, which alter a material's electrical, optical and magnetic properties often dramatically, is one example.[7]

The concept of miniaturization by reducing the size of bulk objects to obtain nano sized structures is termed "top-down" approach. It is basically a combination of physical and chemical processes such as etching and lithography that had been applied for years in the microelectronics, mainly semiconductor, industries. The current state-of-the-art technologies are capable of fabricating silicon nanostructures reliably with the smallest achievable feature size of ~14 nm, with anticipation of 5 nm in similar quality in less than a decade. However, considering the size of molecules in comparison, this is still far beyond atomic resolution. On the other hand, at this level the complexity of physical system dramatically increases, due to the above mentioned scaling laws, which means

that the top down fabrication strategy is going to reach its limits eventually. Examples of smaller devices are essentially based on "bottom-up" procedures, following the fabrication strategies observed in nature, where more complicated or complex assemblies are formed by spontaneous arrangement of smaller components (self-assembly).[8-9] In fact, plenty of advancements in the nanotechnology field were inspired originally from nature, where highly optimized bottom-up principles can be frequently observed in a multitude of naturally occurring structures, materials and phenomena.

With respect to self-assembly, soft materials are the most relevant systems. The soft matter realm embraces a large variety of materials, ranging from liquid crystals and polymers to biological materials and colloidal systems.[10] Accordingly, this realm offers a broad spectrum of choices to fabricate nanoscale structures by (often nature-inspired) bottom-up strategies.

A highly applicable self-assembled soft matter, which has been repeatedly exploited in the past as inspiration for biomimetic device development, is the membrane of the biological cell. Native cell membranes serve as a vital element in various cellular functions. They are essentially two-dimensional fluid supramolecular self-assembly of lipid moieties that are naturally occurring in different part of the cells. The process of membrane self assembly can be modeled and, to some extent, recreated in vitro, where various forms of artificially generated membranes, such as vesicles, solid supported bilayers, and lipid nanotubules, have been produced.[11-15]

The model biomembranes are typically self-assembled from individual lipid molecules upon transfer from an organic to an aqueous solvent environment. Such membranes represent the native environment for membrane proteins, and host additionally other functional molecules. Efficient fabrication strategies for biomembrane devices are currently intensely sought after, as they are expected to facilitate the development of micro- and nanoscale devices and techniques suitable for membrane protein handling, and the investigation of related pathological conditions in humans.

In recent years, scientists have engaged more extensively in mimicking biology in order to develop fabrication methods for new materials and devices. The fabrication of model

systems for light harvesting by using an organizational principle that primitive bacteria employ,[16-18] fabrication of biomimetic imaging sensors inspired by the eye structure in insects,[19-20] and the fabrication of self-cleaning superhydrophobic surfaces by replicating the structure of lotus plant leaves,[21] deserve to be mentioned as prominent examples.

New applications and areas of advance in the life sciences have been emerging continuously. The interface where "bio" and "nano" can meet productively is extensive , which despite great international research efforts remains largely unexplored. An important integrative task in nanotechnology is building the bridge from the macro- via the micro- to the nanoscale. In particular the controlled generation of biomimetic nanostructures using bottom-up methods, which is in nature regulated by proteins, and their use in devices and applications require additional efforts to establish this bridge and render the nanoscale assemblies accessible.

The application of nanoscale devices and tools on biological (living) systems has started to provide solutions for some current problems encountered in medicine and biology. [22] It has also a beneficial effect on the progress in fundamental and applied life science research. In particular the medical applications of nanotechnology, such as nanoelectronic sensors, nanopharmaceutical drug delivery,[23-24] as well as functional nanostructured surfaces on implants, are steadily growing in importance.[25-26]

The core idea of this thesis is built around various fabrication aspects of nanoscale model devices constructed from soft materials, and their integrative aspects. The soft matters of choice are the artificially created, biomimetic membrane, particularly supported monolayers and double bilayers, as well as different embryonic cells, and DNA scaffolds. This thesis introduces several new approaches to manipulate biological membranes, direct them into desired surface areas, and transform lipid material from one type of membrane assembly into another. It will introduce the new fabrication concepts and strategies, briefly discuss experimental considerations and analytical techniques, and finally present ideas for continuation of the research.

2. SURFACES AND INTERFACES

The interaction of soft matter with a solid interface in a fluid environment is considerably influenced by the properties of the surface, for example roughness, surface energy, and surface potential. Determining and understanding these fundamental properties are essential for influencing and controlling the behavior of the investigated soft matter.

In the current chapter, some important physical chemistry aspects of surfaces, which are associated with the work presented in this thesis, are briefly highlighted.

2.1. SURFACE TENSION & WATER CONTACT ANGLE

One of the prominent features of the surfaces is their excess energy. In comparison with the molecules in the bulk of material, the surface molecules have higher potential energy, because they are not completely surrounded by similar molecules at the surface. The net value of this excess energy, surface free energy (F), can be quantified as the forces acting on a unit surface area (Equation 2-1). This also means that to split a solid object into two equal pieces, work (W) has to compensate for the energy stored in the increased surface area (A).

$$\mathbf{F = W/A} \qquad \text{Eq. 2-1}$$

The "surface tension" (γ) is a term used to describe the variation of surface energy with the surface area at constant temperature and pressure (Equation 2-2).

$$\gamma = \mathrm{F} + \mathrm{A}\,\frac{\partial \mathrm{F}}{\partial \mathrm{A}} \qquad \text{Eq. 2-2}$$

In a liquid, the inward rearrangement of the surface molecules, which easily occurs, balances the extra energy to a great extent; therefore F and γ have almost the same value. The formation of a droplet, for example, is due to favorable cohesive forces acting on the liquid surface. However, in solid materials, where surface deformation is restricted, $\frac{\partial \mathrm{F}}{\partial \mathrm{A}}$ is not negligible. Accordingly, the surface energy and the surface tension are not equal.[27]

In this regard, the solid surfaces can be categorized based upon the strength of their internal bonding. Thus metals and glass, for instances, that are composed of strong metallic and covalent bonds, respectively, are considered as high energy surfaces (γ > 500 mN/m), while soft plastic materials like SU-8 and Teflon AF belong to the low energy surface group (γ < 50 mN/m), owed to their weak intermolecular interactions.[12]

One of the common approaches to evaluate the surface tension of solid materials is the measurement of the contact angle of a water droplet placed on the surface. Figure 2-1 illustrates the three balanced tensions at the droplet edge; solid-liquid (γ_{sl}), solid-vapor (γ_{sv}) and liquid-vapor (γ_{lv}), which are correlated to water contact angle (WCA), θ, using Young's equation: (Equation 2-3)

$$\gamma_{sv} - \gamma_{sl} = \gamma_{lv} \cos\theta \qquad \text{Eq.2-3}$$

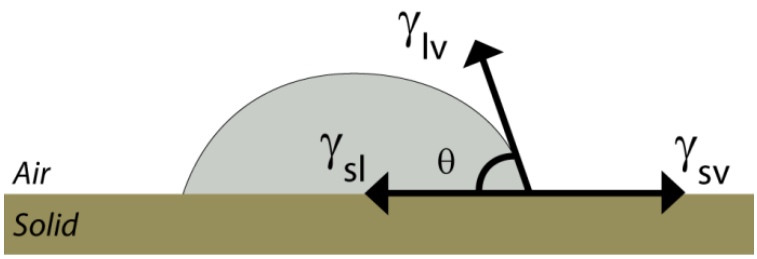

Figure 2-1 Three surface tensions acting upon the edge of a droplet

High energy surfaces usually have WCA < 90°, whilst in low energy surfaces WCA is greater (> 90°). WCA is also considered a suitable index to describe the hydrophobicity, i.e., the surface interaction with water. It is, therefore common to categorize low and high energy surfaces as hydrophobic and hydrophilic, respectively.

Since surface energy is unfavorable, solid materials tend to form new bonds with molecules present at their surface to decrease their excess energy. The adhesion of unwanted molecules on the surface (contamination), and various wetting phenomena can therefore be explained energetically.

2.2. SURFACE WETTING

When a droplet of a liquid is placed on a solid surface, it can, to some extent, cover the surface, and even spread out completely to form a thin liquid film. This process is known as wetting. There are a number of factors that affect the wetting phenomenon. Generally, if the solid-liquid interfacial tension (γ_{sl}) is smaller than the surface tension of the solid (γ_{sv}), the liquid spreads over the surface to decrease its energy, which is referred to as "spreading energy" (Equation 2-4).[28]

$$S = \gamma_{sv} - \gamma_{lv} - \gamma_{sl} \qquad \text{Eq.2-4}$$

By combining equation 2-4 with the Young equation, the spreading energy can be quantified using the WCA (Equation 2-5).

$$S = \gamma_{lv}(\cos\theta - 1) \qquad \text{Eq. 2-5}$$

However, the contact angle is not only affected by surface tension, but also by the roughness of the surfaces. The roughness factor (r) can be simply described as the ratio of actual surface to the geometric surface area.[29] According to Cassie and Baxter, at rough surfaces air can be trapped between the substrate and a fluid droplet, preventing efficient spreading, which results in a bigger contact angle.[30]

The chemical structure of the surface is another factor that affects wettability. The presence of active surface groups, like the hydroxyl group (-OH), alters the electron density and polarity[31] at the surface, which in turn establishes a potential difference known as "surface potential". Kelvin probe force microscopy is a convenient modern technique for measuring this potential (See Chapter 5).

In the presence of an (aqueous) solution with certain ion content and pH, however, the surface charge is sheathed by the accumulation of counter ions in a thin, stagnant layer (Stern layer) at the solid-liquid interface. These ions are brought to the interface through the diffuse layer, where the interchange of ions between the solution and the Stern layer

occurs. The potential difference at the boarder of solution and diffuse layer is known as electrokinetic potential (or Zeta potential) (Figure 2-2).[32]

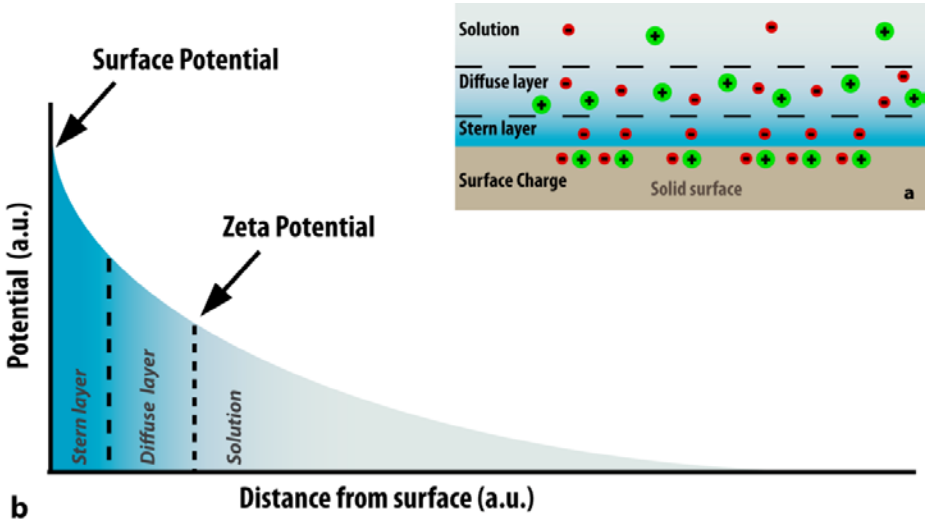

Figure 2-2 a) Schematic representation of the charge distribution at the solid surface and solid-liquid interfaces, showing Stern, diffuse and solution layers, **b)** Potential curve of the solid surface

Both surface and zeta potential can be used as an index to interpret and/or predict the wetting behavior of the interactive liquid (or soft matter) on the surface. The zeta potential of flat surfaces can be measured using indirect electrophoretic light scattering technique. In this method, an oscillating electric field is applied on a probe particle solution (with known charge), which is in contact with the surface under study. The scattering of an incident laser light by the motion of particles results in the frequency shift of light. By measuring this frequency, velocity of the particles can be calculated, which is proportional to the surface charge.

In the current work, the propagation of a lipid monolayer on nanopatterned (low energy) Teflon AF surfaces, and the controlling of lipid double bilayer spreading on high energy Al_2O_3 surfaces, (paper I and IV, respectively), are two examples of wetting phenomena, where a fluid soft matter film spontaneously spreads over the available surface. The associated decrease in surface tension is the driving force for this self-spreading behavior. WCA measurements, roughness analysis, and surface potential measurements have been also used in paper I to characterize e-beam exposed Teflon AF surfaces.

3. PHOSPHOLIPID MEMBRANES

3.1. PHOSPHOLIPID MOLECULES AND SELF-ASSEMBLY

Phospholipids are the main components of biological membranes. As two-dimensional medium, phospholipid membranes can be found naturally in different forms. The bilayer plasma membrane, the monolayer pulmonary membranes, and the neurotransmitter vesicles are some examples of such.[33-34] Transport of membrane intrinsic and associated proteins, assistance in enzymatic reactions, active transport of essential molecules into and out of the cell, and separation of the cell's compartments are among the known functionalities of the biomembranes.[35-36]

Most of phospholipids are composed of two long acyl chains and a polar head group. The acyl chains are typically 16 to 20 carbons long. One chain usually has two carbons more than the other, which along with the existence of unsaturated bonds, introduces an asymmetric structure to the molecule. The acyl (tail) chains are linked to a phosphate (head) group by a glycerol moiety (Figure 3-1).[37]

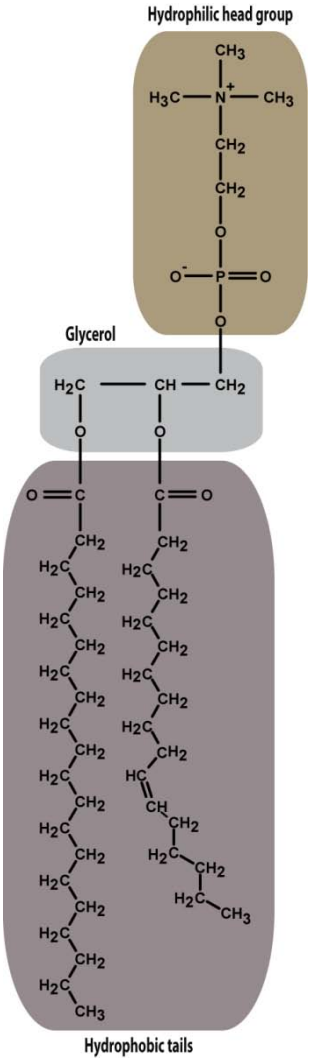

Figure 3-1 The chemical structure of phosphatidylcholine (PC) molecule, which is the major components of biomembranes

Owed to the hydrophobicity of the hydrocarbon tails and hydrophilicity of the charged head group, phospholipids are of an amphiphilic nature, and tend to self-assemble, i.e., spontaneously form organized supramolecular structures, in aqueous solutions. Even though lipid molecules are forming a more organized structure during this process, the driving force of self-assembly is an increase in the entropy of the system.

In an aqueous lipid solution, the water molecules try to align themselves along the hydrophobic tails of lipid to increase the number of hydrogen bonds (hydrophobic solvation). By

adding more lipids in the solution, the number of organized water molecules increases, therefore the entropy of the system declines. Under this condition, lipid molecules rearrange themselves to isolate the hydrophobic tails, accordingly the entropy of the whole system increases since less water molecules are involve in hydrophobic solvation.[38] Equation 3-1 describes the change in free energy of self-assembly, where ΔG is the Gibbs free energy, ΔH is the enthalpy of the system, and $T\Delta S$ is the entropy.

$$\Delta G = \Delta H - T\Delta S \qquad \text{Eq. 3-1}$$

Depending on various factors, like the shape of the lipid molecule, as well as concentration, and temperature of the lipid solution, a range of different self-organized geometries is possible. By controlling the shape of the lipid molecule, the formation of desired structures can be promoted. Particularly the head groups play an important role in defining the final geometries of the assemblies. In this context, a critical packing parameter (CPP) is commonly used (Equation 3-2), where V and L are the volume and length of the hydrophobic tail, respectively, and A is the effective area of the head group.

$$CPP = \frac{V}{AL} \qquad \text{Eq. 3-2}$$

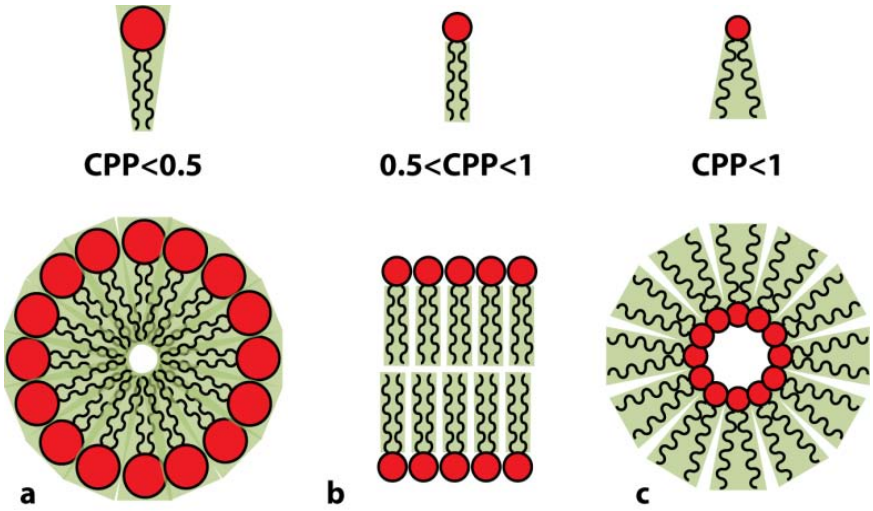

Figure 3-2 Self-organized structures depending on the shape of lipid molecule. **a)** Micelle, **b)** lamellar, **c)** Reversed micelle

Generally, if CPP < 0.5, micelles and hexagonal structures are formed, while in the case of CPP > 1, reversed micelles are the result (Figure 3-2 a and c, respectively). When the volume of head group and tail of a lipid molecule is approximately the same (0.5 < CPP < 1) lamellar structures are the preferred phase (Figure 3-2 b).

The phospholipid molecules in biomembranes, like phosphotidylcholine (PC) (Figure 3-1), phosphatidylethanolamine (PE), and phosphatidic acid (PA), all form the lamellar structure. Due to their structural similarity to plasma biomembranes, lamellar phases are widely used as model systems for biological membranes.[39-40]

3.2. SUPPORTED MEMBRANES

Phospholipids are the main, but not the only constituents of biological membranes. There are also many other molecules present, for example a multitude of different proteins, glycolipids, and steroids, which add to the structural complexity. By providing greater simplicity, better stability and availability on demand, biomimetic membranes, artificially generated from selected lipid components by self-assembly, constitute a versatile substitute. Spherical lipid compartments such as uni- or multilamellar vesicles, and flat supported membranes are examples of model membranes commonly used in biomembrane research.

Introduced by McConnell and Tamm in the 1980s,[41-42] supported lipid membranes have been in the center of attention in different research fields. A large variety of basic and advanced aspects of cell membranes, including mechanical properties, transport phenomena, lipid-protein interactions, and the mechanisms of self-assembly have been studied in the past, having made use of different supported lipid membrane types.[12, 43-44] Moreover, the nano-biotechnological applications of supported membranes are a rapidly growing research field, with special emphasis on biointerface development, biosensing, and membrane protein research.[45-49]

Solid-supported membranes can be formed using the self-assembly route. Aside Langmuir-Blodgett technique in which different types of films can be generated by

transferring the lipid molecules at the air-liquid interface by means of dipping a solid substrate to the solution,[50]there are few other techniques available to supported lipid membranes. Controlled deposition of nanovesicles[51] using a multifunctional pipette[52] to form bilayers, and dip pen lithography with a lipid-coated AFM tip[53] are some examples.

To produce lipid films in this thesis, a relatively new route has been employed in which the propagation of lipid material on surfaces (self-spreading), depending mainly on the surface energy, results in the formation of various types of the supported membranes. High energy surfaces, like glass and metal oxides, promote the generation of bilayer or double bilayer lipid films, where the lipid head groups face both the surface and the (aqueous) liquid (Figure 3-3a and b, respectively). On low energy surfaces like the epoxy polymer SU-8 or the perfluorinated Teflon AF, monomolecular lipid layers are formed, where the tail groups face the plastics surface, and the head groups face the liquid (Figure 3-3c).[12]

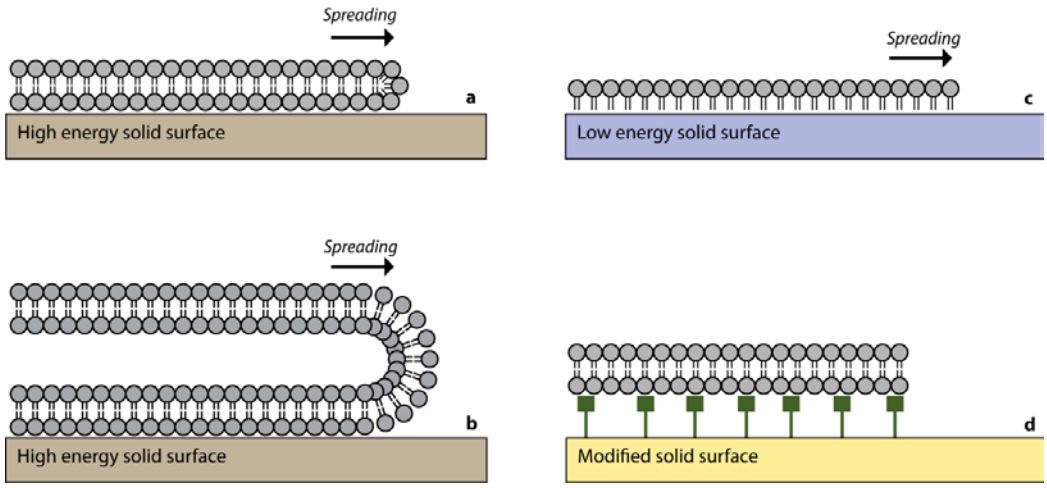

Figure 3-3 Solid supported membranes. **a)** Bilayer, **b)** Double bilayer (flat giant unilamellar vesicle), **c)** Monolayer, and **d)** Tethered bilayer

The driving force of spontaneous lipid self-spreading is the surface tension gradient between the lipid-solid interface ($\gamma_{s\text{-}lipid}$), where the vesicle is deposited, and the solution-solid interface ($\gamma_{s\text{-}Liquid}$) adjacent to it. This phenomenon is known as Marangoni flow.[54-55] Considering the fact that vesicle structure has to rupture to release the lipid material (lysis

tension, γ_{lysis}) the self-spreading (S) happens only if the surface tension gradient is bigger than the lysis tension (Equation 3-3).

$$S = \gamma_{s-Liquid} - \gamma_{s-Lipid} - \gamma_{lysis} \qquad \text{Eq. 3-3}$$

Tethered (or cushioned) bilayers (Figure 3-3d) are another form of supported membranes. Here, a spacer layer is introduced in between the (appropriately functionalized) surface and the self-assembled molecular lipid film. The engineered gap between membrane and surface is beneficial for incorporation of membrane proteins.[12] In comparison to the other supported membrane types, tethered bilayers show reduced two-dimensional fluidity after deposition, which actually limits their effectiveness, in some extent, for membrane protein studies.

The biomimetic membrane part of this thesis relies on the deposition and manipulation of supported membranes, specifically monolayer and double bilayer films, by applying the MLV deposition and self-spreading technique. In paper I it is shown that the spreading process of a lipid monolayer can be controlled on patterned Teflon AF surfaces, and in fact guided through lithographically defined nanolanes, where the special behavior of the lipid film in highly confined spaces was investigated. In paper IV, a lipid double bilayer film on an Al_2O_3-coated surface was manipulated with an IR laser induced temperature gradient, leading to the formation of long and stable lipid nanotubes.

3.2.1. PATTERNING OF LIPID MONOLAYERS ON TEFLON AF

As introduced in the last section, upon the deposition of a multilamellar vesicle on a low energy surface, the lipid molecules cover the interface and form a monolayer film (Figure 3-3c). According to Czolkos et al., the spreading occurs in a circular fashion with the MLV at the origin. The spreading coefficient β can therefore be measured by calculating the radial velocity of the spreading front ($\frac{dR}{dt}$) and the radius of the vesicle (R_0), using equation 3-4, where R is the radius of spreading.[56]

$$Rlog\left(\frac{R}{R_0}\right)\frac{dR}{dt} = 2\beta \qquad \text{Eq. 3-4}$$

Supported lipid monolayers can serve as membrane model for their biological equivalents. The monolayer films in pulmonary system that assist the inhalation and exhalation,[44, 57] and monolayer lipids in the tear film that protects the eyes from drying,[58-59] are some examples of vital functionality of biological lipid monolayers.

Even though most biomimetic membrane research has been, and continues to be, focused on lipid bilayers, which is the natural environment for membrane proteins, the pattering of supported lipid monolayers to fabricate nanofluidic devices has recently gained some attention. Supported lipid monolayers are quite tolerant with respect to external solution conditions, which along with the superior long-term stability of low energy surfaces constitute practical advantages over other supported membrane assemblies.[13, 60] Moreover, higher spreading velocities, as compared to bilayers under comparable conditions ($\beta_{monolayer} \approx 1.7\ \beta_{bilayer}$), [15] is another distinguishable feature of monolayers.

Recently, the application of nano/micro-patterned SU-8 surfaces as nanofluidic substrate for mixing lipids in monolayers,[48] and for controlled release of DNA molecules from decorated surface areas,[61] have been reported, where the spreading coefficient of a lipid monolayer on SU-8 was calculated as 1-3 $\mu m^2/s$. In another study, patterned EPON 1002F (an aliphatic epoxy polymer) surfaces have been applied as a substrate to control the hybridization of two complementary single strands of DNA molecules, conjugated on two different lipid monolayer patches.[62] However both SU-8 and EPON exhibit rather strong auto-fluorescence, which limits their application in biological studies involving common fluorescence-based imaging techniques.[63-65]

Although there is a wide variety of readily accessible low energy surface materials, Teflon AF has recently received special attention as a substrate for fabrication of supported lipid monolayers (cf. chapter 4).[60, 66] Major benefits for microscopy studies on Teflon AF surface are the facile deposition as thin film on many solid substrates, great optical transparency and negligible auto-fluorescence in comparison with SU-8 and EPON, which makes it a superior choice as substrate for lipid monolayer devices in the context of microscopy and spectroscopy.

A comparative study of lipid spreading behavior on SU-8 and Teflon AF revealed some characteristic differences. The spreading coefficient on Teflon AF is 12-20 $\mu m^2/s$, which is about on order of magnitude greater than what was determined for SU-8 (1-3 $\mu m^{2/}s$). This has been related to the lower friction coefficient of lipid molecules on Teflon AF. Moreover, unlike SU-8, which promotes a sharp and distinguishable spreading edge, the spreading edge on Teflon AF is fuzzy (thinning effect). Considering the low friction coefficient and faster spreading on Teflon AF, the fuzziness of the spreading edge is a result of two-dimensional "evaporation" of lipid molecules located at the spreading front onto adjacent parts of the surface.[56]

In this thesis, the spreading behavior of lipid monolayer films in confined nanoscale areas on patterned Teflon AF surfaces has been investigated. The patterns were generated by the direct exposure of Teflon AF with electron beam radiation. The detailed specifications, characterization data and process descriptions of the patterning technique are discussed extensively in chapter 4.

In brief, the e-beam causes decreased hydrophobicity of the exposed areas (WCA = 95°), as compared with unexposed Teflon AF (WCA =118°). Roughness and surface charge become altered as well, resulting in a smoother surface with surface potential difference of 120mV.

It is shown that the spreading of lipid monolayers, which is regularly observed on untreated Teflon AF films, is not supported by e-beam irradiated Teflon AF surfaces (Figure 3-4). It is important to note that even though the exposed regions are still quite hydrophobic, they possess a much smoother surface. This is in contrast to the findings of Czolkos, who stated that lower roughness supports the spreading of monolayers.[56] His conclusion was based on the observation that the lipid spreading does not occur on rough hydrophobic fluorinated carbon polymer surfaces (WCA of 115°), but is easily achieved on comparatively smooth EPON surfaces with a WCA of ~70°.

Apparently, in the case of exposed Teflon AF, hydrophobicity has a stronger influence than roughness. Moreover, the increased repulsion between the bulk negatively charged membranes in the initially deposited MLV, and the electron-saturated, i.e. negatively

charged, surface hinder vesicle rupture, even though the energy gain obtained from wetting would most likely exceed the vesicles' lysis tension.

Relying on this specific lipophobic feature of e-beam exposed Teflon AF, membrane devices can be fabricated. The lipid spreading front is obstructed and confined in enclosed areas on the Teflon AF surface, where the e-beam irradiated regions work as functional barriers. Figure 3-5 illustrates the concept of a lipid monolayer device based on the frame exposure confinement strategy.

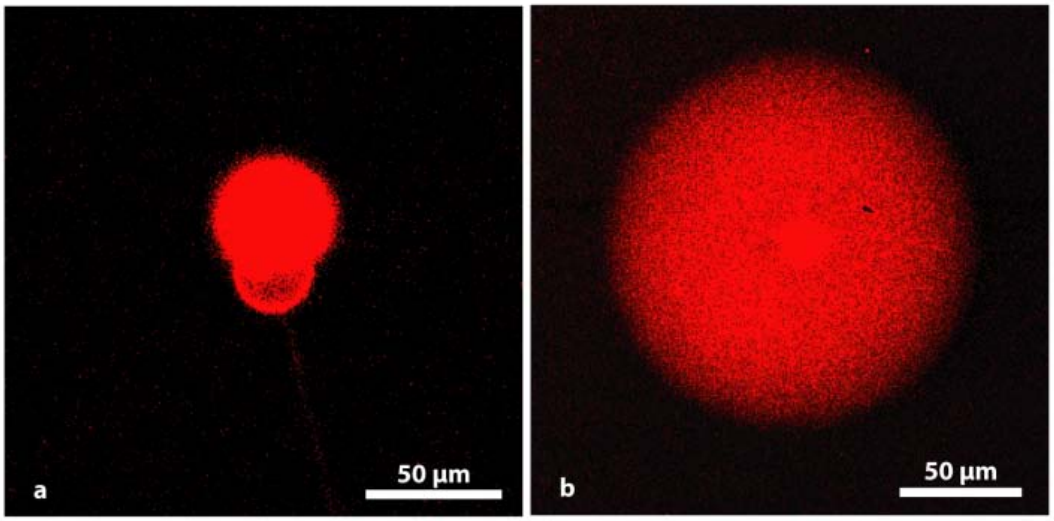

Figure 3-4 a) Multilamellar lipid vesicle deposited on an e-beam-exposed Teflon AF surface. No spreading was observed after 2 h, **b)** A multilamellar lipid vesicle spreads within 5 min after it is deposited onto the Teflon AF surface. (Confocal micrographs of fluorescently labeled lipid material)

When a MLV is placed onto the center of the depicted device (Figure 3-5a), spreading commences instantaneously in a circular manner, until the film reaches the e-beam exposed frames, i.e., the regions depicted in black in the figure. The spreading comes to a halt at this point, and instead continues though the lanes, where the lipid film eventually fills the pools at the end of each lane.

By doping a small percentage of the multilamellar lipid source (1%) with fluorophores, the spreading procedure can be monitored using the confocal microscopy technique (Figure 3-5b).

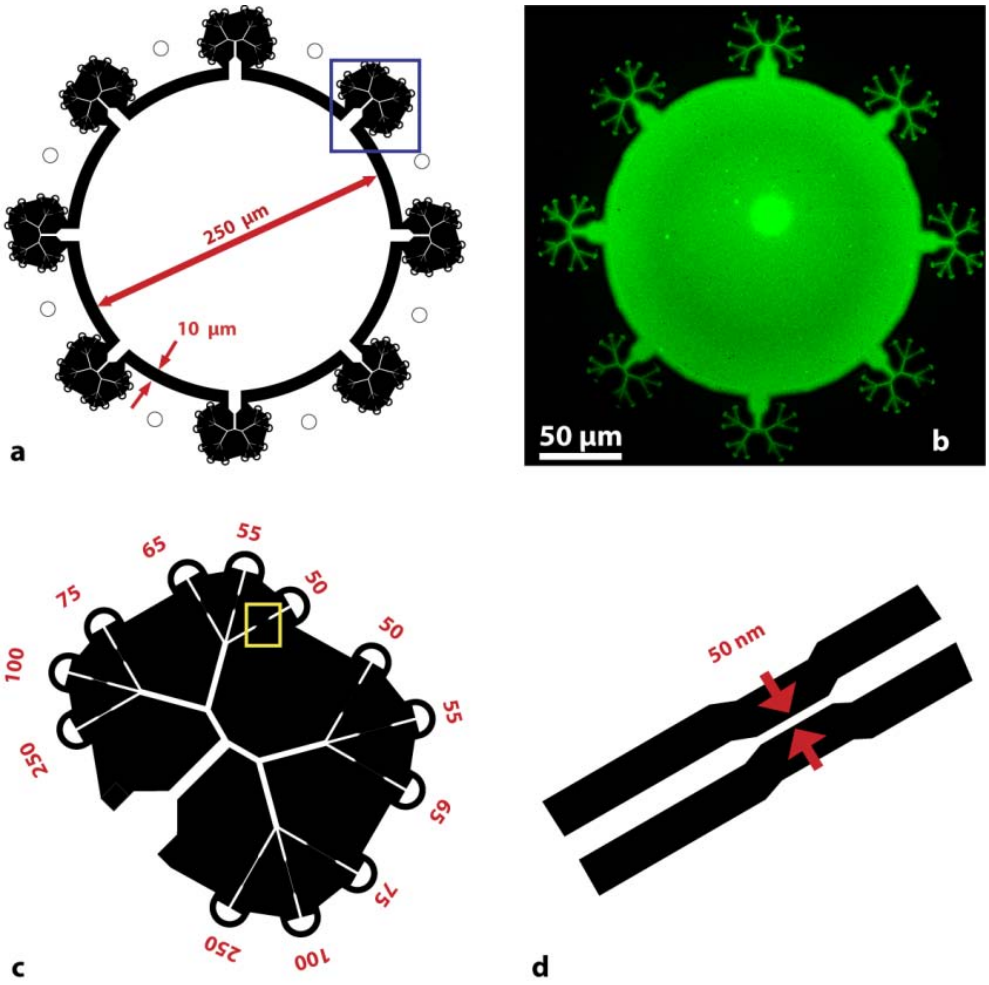

Figure 3-5 a) The design of a lipid spreading device suitable to observe the behavior of lipid films in confined 2D geometries. The black areas represent regions exposed by an electron beam, **b)** Confocal image of the entire structure of lipid spreading in device, recorded after 185 min**, c)** Enlarged view of one of the branches (blue square in panel a). The numbers in the drawing denote the designed width of the corresponding nanolanes, **d)** Close-up view of the smallest, 50 nm wide, lane (yellow square in panel c).

At lane widths above 65 nm, the end pools fill nearly equally fast (Figure 3-6a and b). Below 65 nm, however, the required time for filling the pools increases dramatically from a few minutes to hours. In the constricted areas, surface adhesion energy (σ_{adh}) competes with the sliding friction between the Teflon AF surface and the lipid film (ζ).[48] Even though there is still an energy gain derived from wetting, flow resistance increases and slows down the process.

Based on equation 3-5, the spreading coefficient of a lipid monolayer can be quantified as:

$$\beta = \frac{\sigma_{adh.}}{2\zeta} \qquad \text{Eq. 3-5}$$

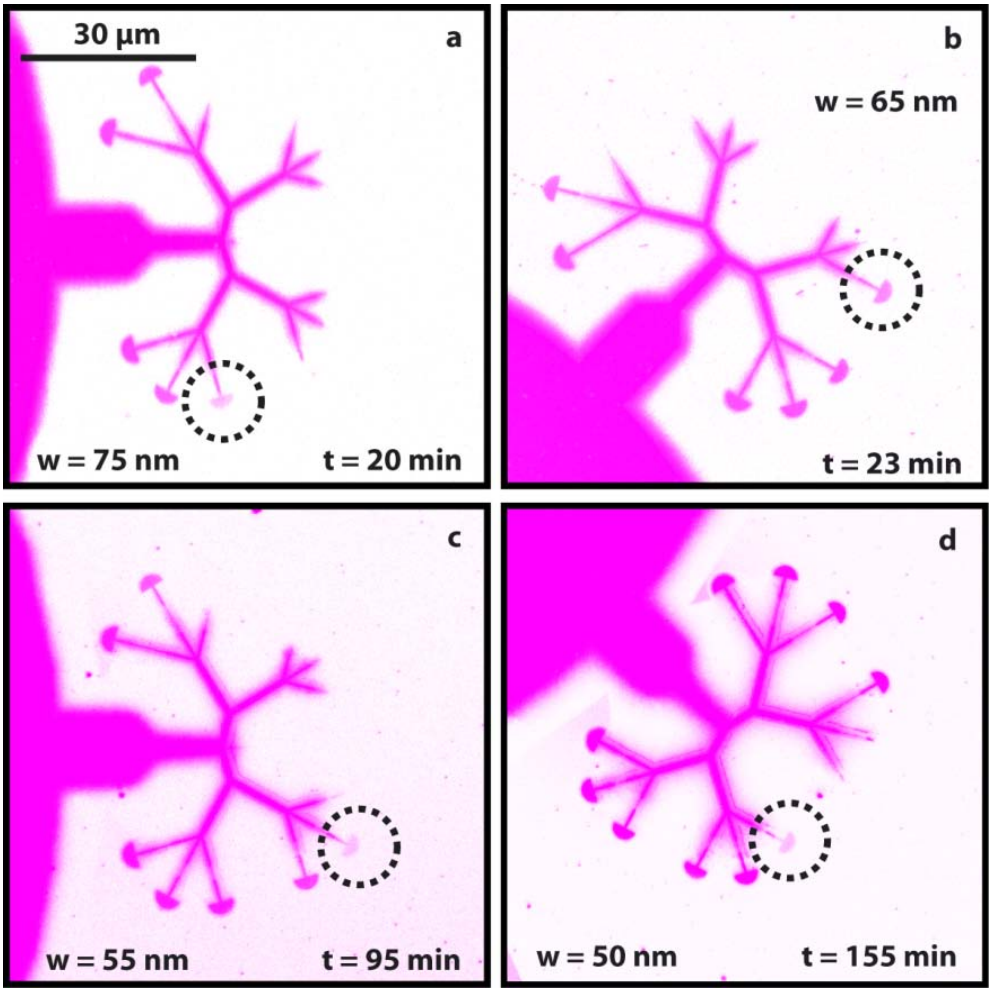

Figure 3-6 Confocal image of one of the branches of the pattern depicted in Figure 2, demonstrating the lipid spreading in Teflon AF areas confined by e-beam exposure. The images were recorded at different time intervals after deposition of the MLV, **a)** 20 min, **b)** 23 min, **c)** 95 min, and **d)** 155 min. The lipid was doped with the fluorophore ATTO 488 (1% w/w). The dotted circle highlights the end pool which has just been filled at the time of recording. The images are inverted for better contrast.

In this model, however, the boundary energies have not been considered. The boundary energy is relatively weak for large area films, and therefore it is negligible for lipid film spreading on micron-sized lanes.[61] But in a case where the film boundary to area ratio

becomes large, it may become important. In the case of spreading in a lane, the surface energy is calculated as:

$$E = -\sigma_{adh.} wL + 2\gamma_e L \qquad \text{Eq. 3-6}$$

where w is the lane width, L the lane length, $\sigma_{adh.}$ the adhesion energy, and γ_e the edge tension (boundary energy). Considering equation 3-5, the spreading coefficient for a lane can be written as:

$$\beta = \frac{\sigma_{adh.} - 2\gamma_e/w}{2\zeta} \qquad \text{Eq. 3-7}$$

which shows the dependency of the spreading on the lane width. At a critical width ($W_{crit.}$) of the lane (Equation 3-8), when the energy gain from wetting is equal to the energy loss induced by the edge tension of the lipid film, the spreading is no longer energetically favorable. Therefore, if w approaches $w_{crit.}$, spreading will slow down significantly and must eventually stop.

$$w_{crit.} = \frac{2\gamma_e}{\sigma_{adh.}} \qquad \text{Eq.3-8}$$

Assuming that γ_e of the monolayer is of the same order of magnitude as the edge tension of bilayer membranes (1-50 pN) and that $\sigma_{adh.}$ of Teflon AF is larger than the lysis tension of the reservoir (1-10 mN m^{-1}); the $w_{crit.}$ of the current membrane device is on the order of a few tens of nm ($w_{crit.}$ =10 nm for $\gamma_e = 25\ pN\ and\ \sigma = 5\ mN\ m^{-1}$). Note that the spreading in the abovementioned device did not stop, but slowed down to a great extent at w=50 nm. It is therefore reasonable to assume that the critical lane width lies somewhere between 10 and 50 nm.

However, there are also other factors that can slow down the lipid spreading at nanolanes. Surface roughness and local defects are some examples of such. The membrane viscosity, which is usually insignificant on the micrometer scale, is another element that very likely has a more pronounced effect of the spreading of monolayers at critical widths. In this

context, the characteristic length (L_c) is used to describe the cross-over scale, i.e., the width of the constriction where the membrane viscosity becomes more important than sliding friction (Equation 3-9).

$$L_c = \sqrt{\frac{\eta}{\zeta}} \qquad \text{Eq. 3-9}$$

where η is the 2D velocity of the lipid film and ζ is the surface-monolayer friction. If there is pinning to the lane edge, the 2D film viscosity can play a role. If there is no pinning to the edge, the 2D viscosity is irrelevant, because the flow of surfactants will be a "plug flow", i.e., featuring no shear, and no viscous dissipation.

Although the spreading over e-beam exposed areas is initially not favorable, it competes with the spreading in the confined nano lanes when the critical width is approached. Figure 3-7c shows the propagation of lipid film crossing the boundary frames, where the fuzziness of the borders increases while the newly filled lanes remain sharp at the edges (arrows 1 and 2 in figure 3-7c, respectively).

Since the e-beam exposed areas are more hydrophilic in comparison with unexposed Teflon AF, one can assume that the formed lipid film on exposed frames is of bilayer nature. However, further observations revealed that the fluorescence intensity of the film at the frame is higher than for the membrane spreading on unexposed Teflon AF, but only by a factor of ~1.5 (Figure 3-7a-b), which excludes the possibility that the monolayer folds into a bilayer, since in this case the measured fluorescence intensity would be twice as high as the monolayer intensity.

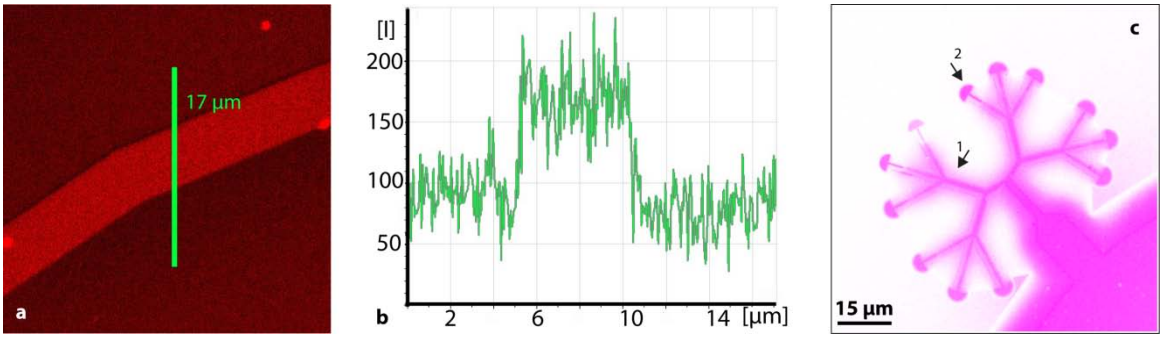

Figure 3-7 a) Higher fluorescence intensity at the e-beam exposed frame, **b)** The intensity profile from (a), **c)** Magnified view of one of the branches after 185 min of spreading time. Arrows 1 and 2 point to the

fuzzy, and the sharp edges of the lipid film spreading on the exposed area and in the newly filled end pools, respectively.

Moreover, the geometry of the patterns in this membrane device as well as its fabrication parameters play crucial roles in the successful patterning of the monolayer film. It is shown that a minimum e-beam dose of 1125 μC/cm^2, along with a minimum frame width of 10 μm are required to guarantee the blocking of lipid spreading efficiently. It is especially important if it is desired to separate spreading lanes from each other as the cross-contamination can effectively be avoided by designing the pattern to leave a large enough distance between individual spreading areas.

There are still several important elements that need to be addressed, regarding the development and characterization of this novel membrane device. Questions like whether the dye label interacts in some way with the exposed surface, and gets concentrated there, as well as the effect of dye charge and size on the behavior of the system, for instance, require further investigations.

3.2.2. FABRICATION OF NANOTUBES

One of the morphologies in which self-assembled lipid bilayer membranes can exist is a hollow (buffer-filled) tube (Figure 3-8). Known as lipid nanotube, this long cylindrical structure has a diameter (*d*) between ten to several hundred nm, depending on lipid composition. The length (*l*) is practically only limited by the available lipid material.

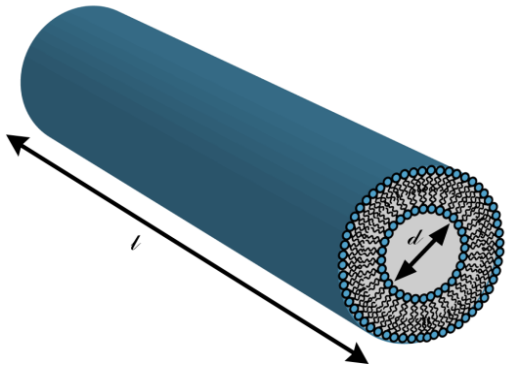

Figure 3-8 Lipid nanotube segment with cross section. The wall of this cylindrical structure typically consists of a single bilayer membrane. The picture is not drawn to scale. *L* and *d* stands for length and diameter, respectively.

The first report on the occurrence of lipid nanotubes in between mammalian cells[67] dates back to 2004, shortly after, the artificially generated nanotube-vesicle networks had been introduced.[68] Even though membrane nanotubes are commonly observed *in vitro* in cultures of many different cell types, it is still not entirely clear whether they also exist *in vivo*. It remains a challenging goal to understand how long-range chemical and information transport between cells is organized, and to what extent nanotubes contribute.[69-70]

Reports on the use of lipid tubes in nanoscale devices are still rather rare, but the interest in bottom-up strategies for fabricating such devices has been growing rapidly.[71-74] The possibility to transport cargo through the flexible lipid conduits make them potentially useful in bioinspired sensing and computation devices, as well as ultra small chemical reactor networks.[75-76] The few existing examples of such miniaturized soft matter reactors interconnected by nanotubes were challenging with respect to fabrication, requiring mechanical action with micromanipulators and glass microneedles to transform the membranes of liposomes into nanotubes.[63, 68] It had not been possible thus far to fabricate lipid membrane nanotubes in such interconnected systems by more common nanofabrication methods.

The energy barrier of nanotube formation, when starting from membranes, is quite high (~ 10 pN).[77] This is due to the high bending curvature at the membrane-tube junction, so that the nanotubes can be generated only if a highly localized load is applied on a lipid membrane. The motor proteins like myosin, that convert chemical energy into a mechanical force, are thought to be one of the possible stimuli responsible for nanotube creation in cells.[70, 78] In vitro, the localized force can be a hydrodynamic flow, mechanical manipulation with micropipettes, and optical or magnetic tweezers[79-80]. If a mechanical force is applied, for example by means of a glass micropipette to surface-immobilized giant unilamellar vesicles connected to a membrane source, tubes are generated, and terminated with a new vesicle, which derives its membrane material from the lipid reservoir by Marangoni flow. Thus, small networks of nanotube-interconnected membrane containers can be fabricated.[69, 81] One recently reported alternative approach to nanotube generation involves the curvature generating abilities of nanoparticles, which

have been encapsulated in lipid double bilayer membranes. This artificial system produced spontaneous nanotubes in large numbers, and showed some resemblance to the action of virus particles in biological cells. [82]

In the work presented in this thesis (paper IV), a lipid double bilayer patch was manipulated by applying a local temperature gradient to generate networks of lipid nanotubes and flat giant unilamellar vesicles (FGUVs).

The double bilayer membrane was formed by the deposition of a MLV on a high energy surface (Al_2O_3-coated glass), where the self-spreading of the MLV on the surface generates the supported lipid film (cf. Figure 3.3.b). Note that the formation of bilayers on hydrophilic high energy surfaces is strongly dependent on the ionic strength of the surrounding aqueous buffer.[83-84] This is due to the high density of hydroxyl groups, which in turn elevates the negative charge of the surface (cf. chapter 2). Thus the presence of divalent cations like Ca^{+2} and Mg^{+2} in low concentrations, in particular, promotes the formation of double bilayers on the surface,[85-86] as they facilitate the adhesion of the lipid film by screening the negative charge of both the surface and the lipid. [87] The surface tension gradient is the driving force for spreading of this type of lipid film, too. The thin layer of ions immobilizes the lipid layer in the vicinity of the surface; therefore it is believed that the spreading of the double bilayer occurs by the sliding motion of the upper bilayer, which rolls down toward the surface in a tank thread-like motion (Figure 3-9).[86]

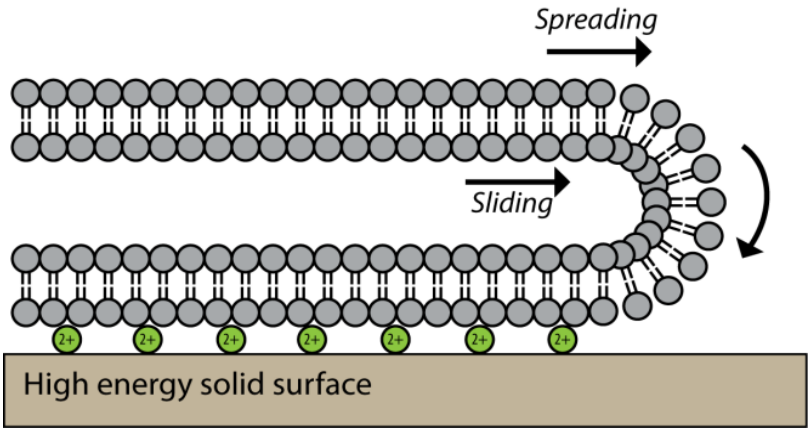

Figure 3-9 The spreading mechanism of double bilayer membrane. The lower bilayer is immobilized on the surface by cations. Spreading occurs by a combination of sliding motion of upper bilayer and rolling of the edge.

As a result, a thin water layer of ~100 nm separates the two stacked bilayers, which is completely encapsulated. Therefore, the double bilayer can be viewed as a flat giant unilamellar vesicle (FGUV).

When a local temperature gradient is created on a part of a FGUV the surface adhesion energy decreases, resulting in local de-wetting of the surface. Accordingly, a portion of exposed lipid molecules, in the form of a small vesicle, separates from the source and migrates along the generated adhesion gradient, known as thermomigration. Interestingly, it is leaving a nanotube behind. By either moving the location of the temperature source (a focused IR-B laser in this case), or moving the substrate while the heat source is fixed at its position, a network of nanotubes that interconnect double bilayer patches separated from the main membrane area, can be fabricated (Figure 3-10).

Figure 3-10 Graphically enhanced representation of nanotube formation induced by thermomigration. The star shows the location of the IR-laser. The double bilayer membrane initially covered the entire visible area, and was driven apart by thermally induced de-wetting, forming the nanotubes in the process.

Microfabrication techniques can be applied to pattern the surface, establishing a simple framework for guiding the nanotube formation. In the case presented here (paper I), an array of SU-8 corridors have been fabricated on a glass substrate. The patterned surface was coated by a thin layer of oxidized aluminum prior to the deposition of the MLV (Figure 3-11).

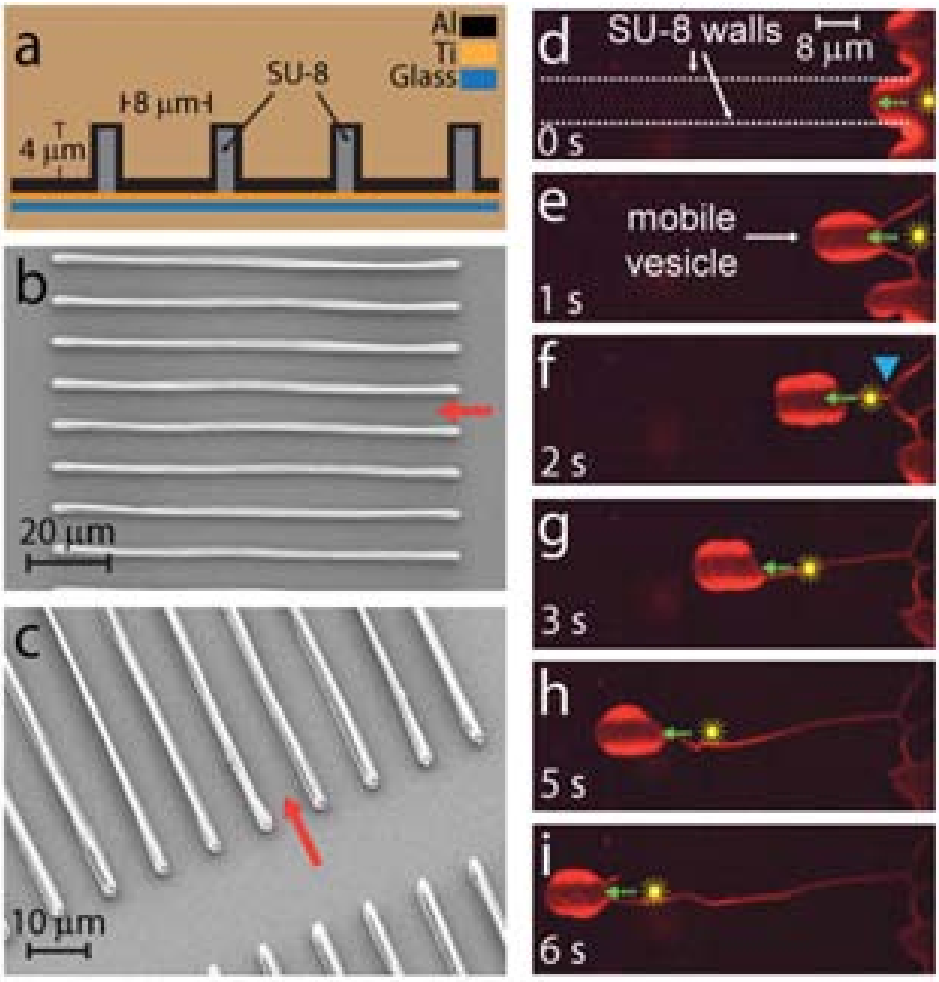

Figure 3-11 Directed thermomigration of mobile vesicles and formation of nanotubes. **a)** A schematic of the cross sectional view of fabricated surfaces. **b–c)** Scanning electron micrographs (SEM) of the SU-8 corridors in top and perspective view, respectively. The red arrows indicate the entrance of the corridors. **d-i)** The entry of a mobile lipid vesicle into an SU-8 corridor. The wall positions are marked with white dashed lines. The location of the IR-laser spot is marked with a yellow star, and the direction of its translation with green dashed arrows. e) Separation of the mobile vesicle from the bulk film, as it enters the corridor. The vesicle is confined inside the walls. **f–i)** Migration of the mobile vesicle, leaving a trailing nanotube behind. The blue arrow head in (f) points to a Y-junction between the lipid nanotubes formed in the process.

This unconventional contact-free fabrication method of nanotubes is an example of soft matter nanofabrication, where the combination of conventional top-down lithography with the self-spreading bottom-up strategy leads to a versatile membrane device. It provides a facile means of fabricating lipid nanotubes on-demand. The particular strength of this technique is the ability to easily generate a new kind of vesicle-nanotube network, which has significant advantages over the earlier reported networks produced by the microneedle technique.[68]

4. PATTERNED TEFLON AF SURFACES

A major share of the work presented in this thesis has been performed on substrates coated with the amorphous fluoropolymer Teflon AF®, therefore a separate chapter has been dedicated to discuss thoroughly the properties of Teflon AF and related procedures.

Introduced in 1989 by Du Pont, Teflon AF (TAF) is the trade name for poly-(4,5-difluoro-2,2-bis- (trifluoromethyl)-1, 3-dioxole-co-tetrafluoroethylene), the final product of copolymerization of tetrafluoroethylene with (2, 2-bis-trifluoromethyl-4, 5-difluoro-1, 3-dioxole) PDD (Figure 4-1).[88]

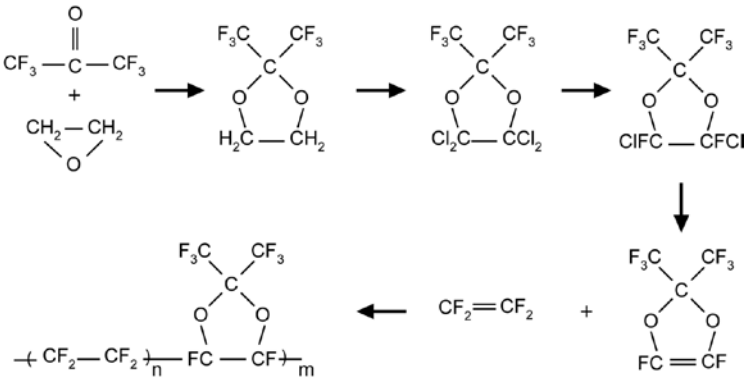

Figure 4-1 Chemical synthesis of Teflon AF

Like all other members of the perfluoropolymer family, i.e., polymers in which all the hydrogen atoms have been replaced by fluorine, TAF has excellent thermal stability, chemical inertness, and low surface energy, owed to the strong C-C bond (607 kJ/mol) and the special nature of the C-F bond (507 kJ/mol). Due to the high electronegativity of fluorine, the C-F bond has ionic character, which causes an electron sheath around the C-C bonds in the backbone of the polymer. This protects them against decomposition by chemical reagents and thermal breakdown processes.[89-91] In contrast to other fluoropolymers, which are semicrystalline, TAF has an amorphous structure. It is optically transparent down to 200 nm in wavelength.[92] The existence of dioxole groups in the structure of TAF distinguishes it from similar perfluoropolymers, adding beneficial properties like increased solubility in some perfluorinated solvents.

Besides the weak van der Waals interactions in TAF, which inhibit the perfect packing of chains in the amorphous regions, the high rotational barrier of the dioxole group (60 kJ/mole)[64] causes large spaces between the polymer chains (free fractional volume, FFV)

with a cavity size of 12-16 Å. This allows for high permeability for gases and some solvents through thin films of the polymer.[93] Many properties of TAF depend on the ratio of its monomers in the structure (Table 4-1). For example, its solubility in fluorinated solvents decreases with an increasing share of PDD. Commercially, there are two grades available; Teflon AF 1600 (glass transition temperature (T_g) of 160°C) and Teflon AF2400 (T_g of 240°C), that contain 64 and 83 mol % of PDD, respectively.

Table 4-1 Key properties of Teflon AF

	Teflon AF 1600	***Teflon AF 2400***
Dielectric constant	1.93	1.89
Optical transmission	>95%	>95%
Refractive index	1.31	1.29
Tg (°C)	160	240
Volume coefficient of thermal expansion (ppm/°C)	280	300
Gas permeability O_2 (Barrer)	340	990

In addition to applications of TAF as a protective coating layer, [94-95] TAF is used in electronics as an efficient insulator,[96-98] especially because it possesses one of the lowest dielectric constant (1.89) of all known solid polymers.[90, 99]

Relying on the high FFV and chemical stability, TAF films have been widely applied as membrane in chemical analysis of binary mixtures of chlorinated hydrocarbons,[2] carbondioxide/methane or helium,[100] hydrogen/methane,[101] or to detect and filter ozone,[102] as well as oxygen.[103] Moreover, the new generation of waveguide sensors in which the liquid core tube has been coated by TAF, have higher sensitivity in detecting trace amounts of molecules.[34, 104]

Research on TAF in the life science context revealed excellent biocompatibility, and cytophobicity.[105] This led to investigations on TAF as substrates for biomembranes,[66] and cell patterning.[60, 106-108] In comparison with the commonly used epoxy photoresist SU-8, and other typical low energy polymeric surfaces fabricated from materials such as PMMA and EPON, TAF exhibits much lower surface energy (cf. Chapter 2) and very low auto-fluorescence, which makes it a superior choice for biological studies involving fluorescence microscopy techniques.[66, 109]

4.1. PATTERNING OF TEFLON AF

Although the chemical inertness of TAF is considered an advantage in many cases, it causes practical difficulties in micro- or nanopatterning of this polymer. TAF is insoluble in most organic solvents. Current fabrication techniques (Table 4-2) for micropatterning of fluoropolymers, including TAF, are mostly based on etching the material off the surface by means of focused ion beam (FIB), synchrotron radiation (SR), and focused laser beam techniques, all of which achieve resolutions of a few micrometers.[110-114] Standard photolithography methods have also been reported as an alternative, allowing for micropatterning of TAF surfaces with the smallest feature size of ~1-2 µm.[60, 107, 115] Therefore, new fabrication strategies for fabricating patterns on TAF films with smaller features than currently possible have the potential to enable new application areas.

Table 4-2 Summary of available pattering methods for TAF

No	Process/material	Minimal reported feature size	Application	Reference
1	Laser ablation/ PTFE	50 µm	---	*Costela, et.al., J. Appl. Phys,* ***1995*** [110]
2	Photolithography &Plasma etching/ PTEF	5µm	Cell patterning	*Makohliso,et.al., iosensors & Bioelectronics,* ***1998***[107]
3	Photo-etching by SR/ PTFE	80 µm	---	*Katoh,et.al., Sens. Actuator A-Phys,* ***2001***[113]
4	Micro molding/ Teflon AF	2µm	Ion channel recording on lipid bilayers	*Mayer,et.al., Biophys. J,****2003***[115]
5	E-beam patterning/ Teflon AF	200 nm	3D lithography	*Karre, et.al., IEEE Trans. Nanotechnol,****2009***[116]
6	Microcontact printing / Teflon AF	1-2- µm	Cell patterning	*Valle,et.al., Advanced Engineering Materials,* ***2010***[106]
7	FIB mask-less etching / PTFE	Fibers: 130 nm [1] Fibers: 90 nm [2]	----	*1. Miyoshi,et.al., Radiat. Phys. Chem,****2011***[111] *2. Fukutake,et.al, Jpn. J. Appl. Phys,* ***2010*** [112]
8	Photolithography & lift-off/ Teflon AF	1µm	Mixing of lipid monolayers	*Czolkos, et.al., SoftMatter,* **2012** [60]
9	Thermal molding/ PTFE	500 nm	---	*Kobayashi,et.al., Nucl. Instrum. Methods Phys.,* ***2013***[114]

4.1.1. PATTERNING BY ELECTRON BEAM RADIATION

An alternative technique to fabricate nano-sized patterns on TAF uses direct electron beam irradiation on nanometer-thin films of the polymer. The first report by Karre *et al.*, who applied it to 250 nm-thick layers of TAF on silicon wafers, describes the formation of trenches in the exposed areas with a minimal feature size of ~200 nm.[116] According to their findings, e-beam treatment causes changes in the molecular structure of the material due to chain scission, which is accompanied by the loss of small gaseous compounds, including hexafluoroacetone and acid fluoride radicals.

This technique has been applied in the present work (paper I and II), to fabricate patterned TAF surfaces, where the effect of e-beam radiation on a thin film of TAF has been studied in more detail.

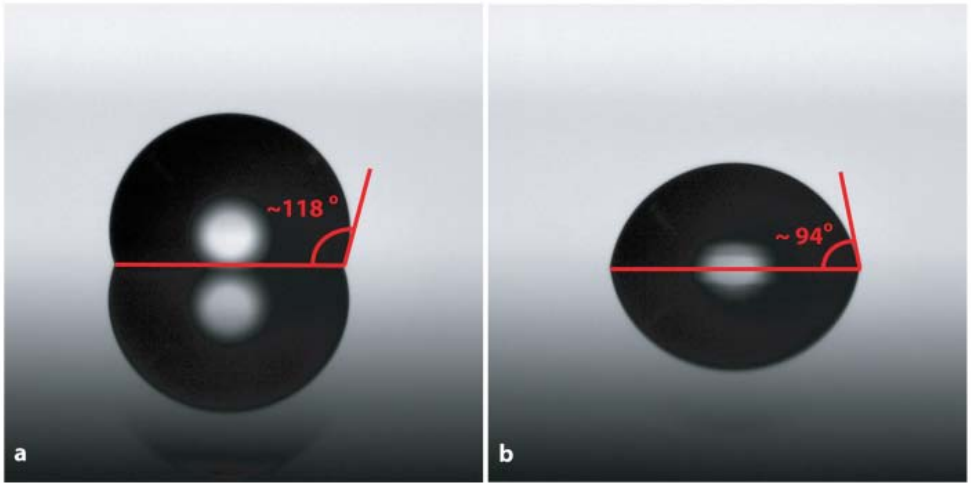

Figure 4-2 Water contact angle measurements on **a)** Plain Teflon AF; and **b)** E-beam exposed Teflon AF

One of the main features of e-beam exposed TAF is the considerable reduced hydrophobicity. This has been shown by water contact angle measurements on as-spun, and irradiated TAF surfaces that indicate a decrease from 118° to 94°, respectively (Figure 4-2).

In addition to hydrophobicity changes, the wettability is affected by the roughness of the surface (cf. chapter 2). Roughness measurements using AFM showed that TAF surfaces become almost three times smoother after being treated by e-beam radiation (Figure 4-3).

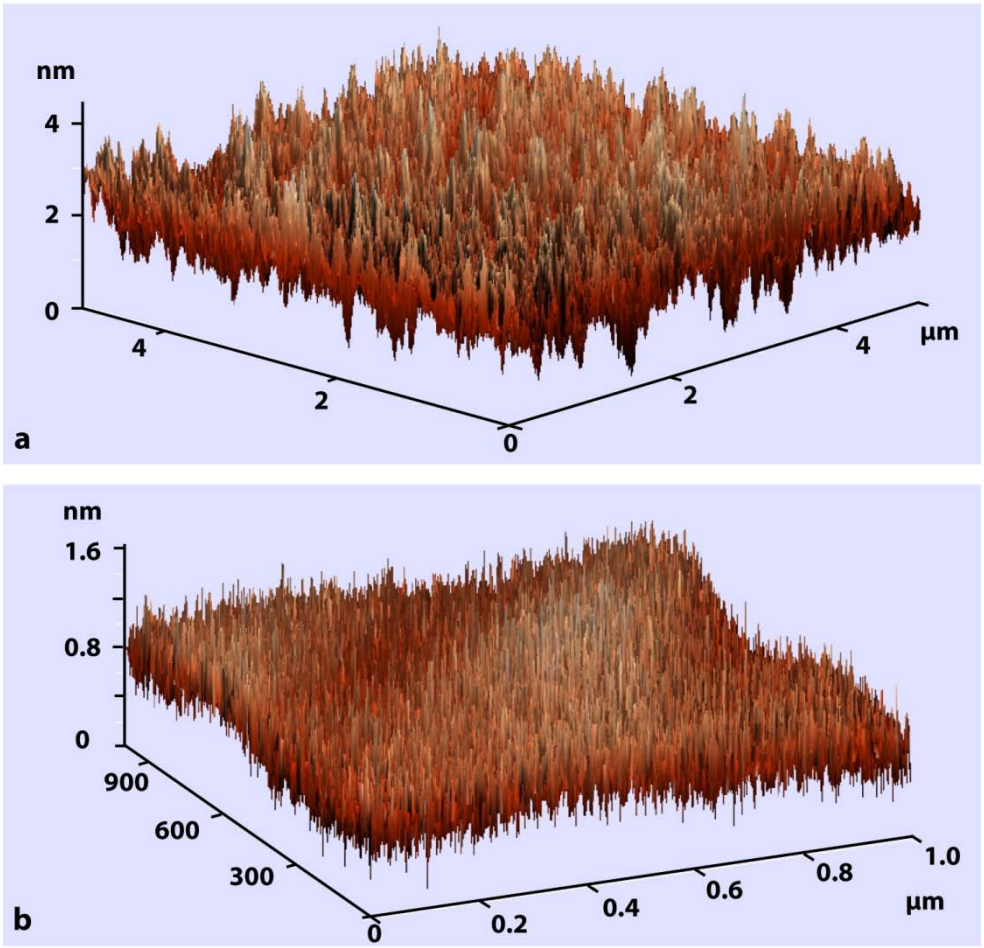

Figure 4-3 AFM images of Teflon AF surfaces roughness before and after exposure to e-beam radiation, **a)** Unexposed Teflon AF, **b)** Exposed Teflon AF. The exposed area has a 3x reduced surface roughness.

The reduced hydrophobicity of exposed TAF surfaces can be explained by the formation of C=O functional groups, due to the degradation of the polymer by e-beam radiation. The latter has been concluded from the appearance of a peak around 535 eV in X-ray photoelectron spectroscopy (XPS) oxygen analysis (Figure 4-4). There are in fact other studies that question the chemical inertness of TAF.[117] Lai et.al, found that this polymer originally contains carboxyl functional groups at very low concentrations. Their observation was based on the potentiometric measurements using TAF as ion selective membrane, where Ca^{+2} ions and unprotonated ionphores showed strong interaction to the membrane. This finding was supported by spectroscopic evidences, suggesting that the carboxyl group is the result of hydrolysis of (C=O)F (acid fluoride) groups in the backbone of the polymer.[118]

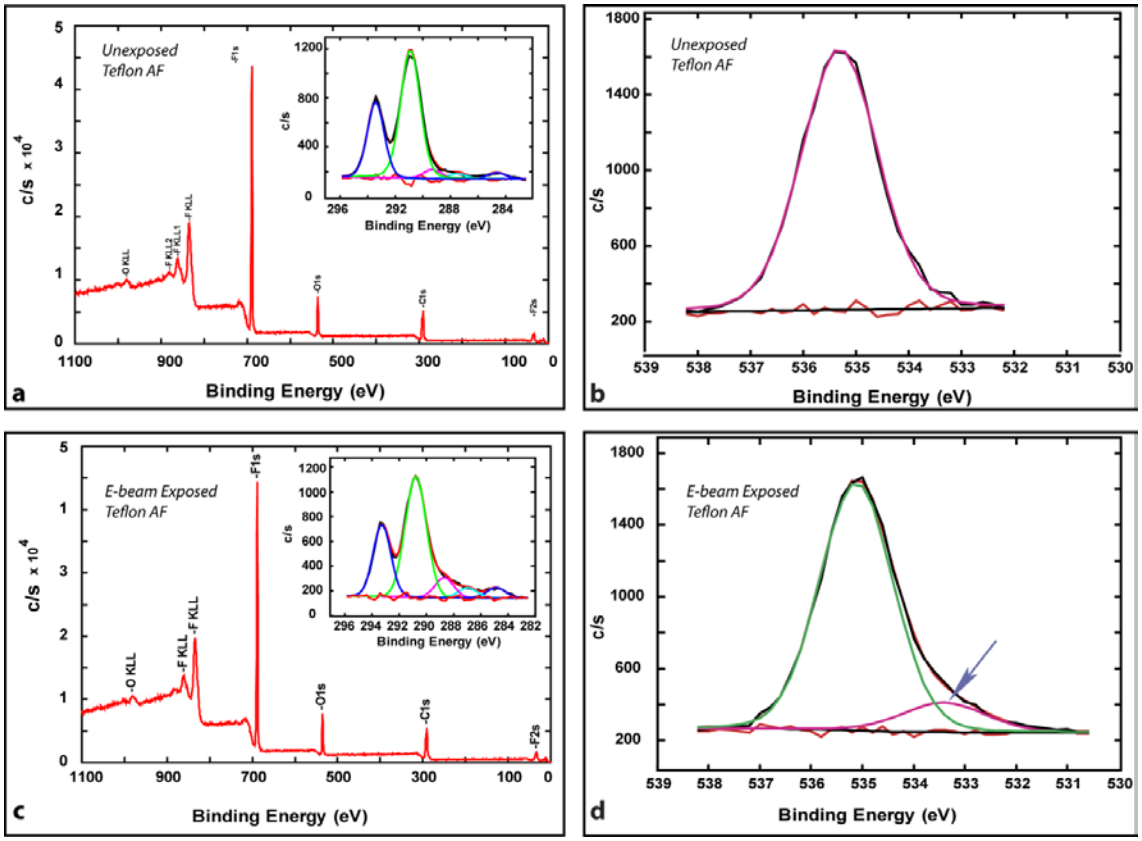

Figure 4-4 a) Carbon XPS spectra of unexposed Teflon AF. **b)** Oxygen XPS analysis of unexposed Teflon AF. **c)** Carbon XPS spectra of e-beam irradiated Teflon AF. **d)** Oxygen XPS analysis of e-beam irradiated Teflon AF.

As mentioned earlier, another noticeable feature introduced to TAF films by e-beam radiation is the formation of dose-dependent trenches in exposed areas (Figure 4-5a). The effect of the applied e-beam dose to the depth of the structure is shown in figure 4-5b. Moreover, according to Karre et.al., the pattern depth is linearly dependent on the initial thickness of the deposited film, i.e., deeper trench structures are formed on thicker film layer under the same exposure conditions.[116]

E-beam lithography inevitably involves the accumulation of electrons in the material, which generates surplus negative charges in the exposed regions. Due to the presence of the polarized C-F bond, TAF is considered as an electret, a material with quasi-permanent dipole polarization, which can keep the applied charges for very long term.[119] The exposure of e-beam radiation with 100kV on ~ 40 nm thick films of TAF generates surface potential differences of about 120mV, regardless of the applied dose (Figure 4-5c).

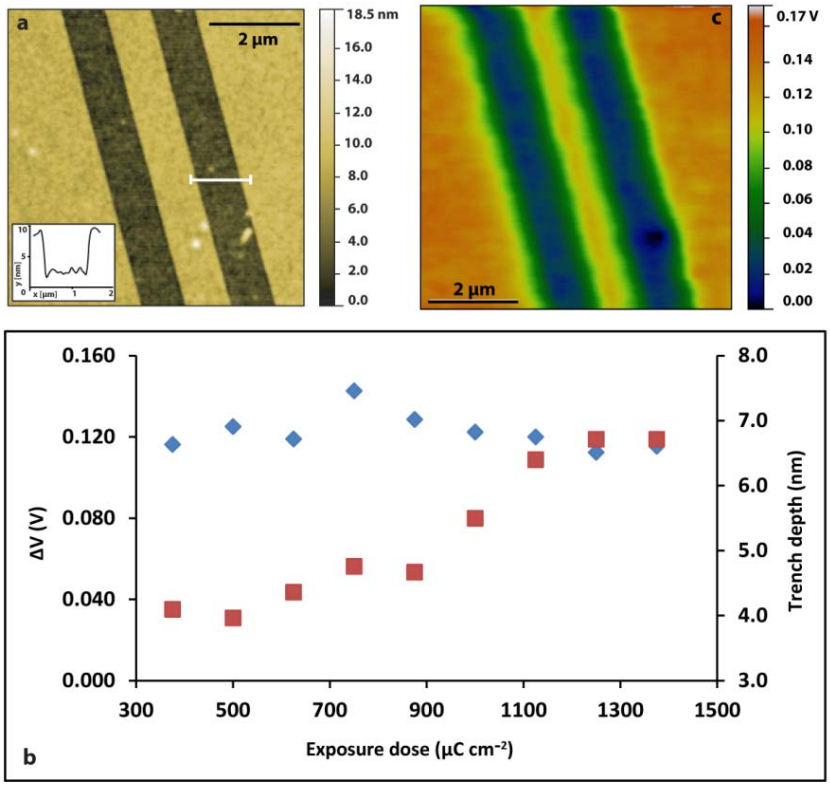

Figure 4-5 a) AFM topography image of the Teflon AF surface after e-beam exposure. **b)** Dose dependency of the surface potential (blue diamonds) and trench depth (red squares). **c)** Kelvin probe force microscopy image of the e-beam-exposed frame.

In paper II, the application of e-beam patterned Teflon AF surfaces as a substrate to guide and pattern different kind of embryonic cells has been investigated (Figure 4-6). This new approach of cell patterning relies on the appearance of more carboxyl groups upon chemical change at exposed areas, which, along with electrostatic interaction, shows strong cytophilic properties to support cell adhesion.

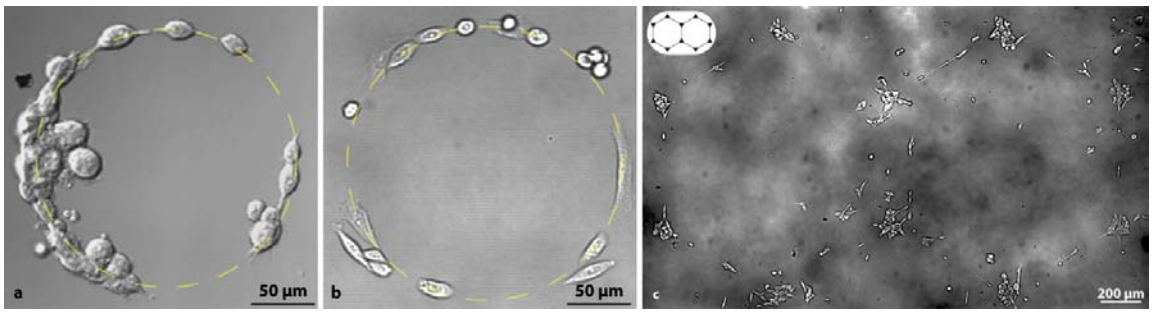

Figure 4-6 Bright field microscopy image of different cell lines on e-beam patterned Teflon AF surfaces, **a)** Human embryonic kidney cells, **b)** adherent Chinese hamster ovary cells, **c)** neuroblastoma cells. The inset shows the outline of the pattern.

4.1.2. PATTERN DEVELOPMENT

An important disadvantage of direct e-beam patterning using the Karre technique is that isolated structures cannot be fabricated on TAF surfaces, as is common with ordinary photo- or e-beam resists. To be able to isolate the exposed pattern, a selective solvent (developer) is required that discriminates between exposed and unexposed regions on TAF.

One of the most recent advancement in this regard has been introduced in our current work (paper III) where it is shown that perfluorinated 2-butyl tetrahydrofurane (Trade name Flurinert FC 75) dissolves TAF, but not the exposed areas, and can therefore be used as developer to complete the lithographic procedure, achieving nanometer resolution. Figure 4-7a and b show AFM images of exposed TAF before and after applying FC75, respectively.

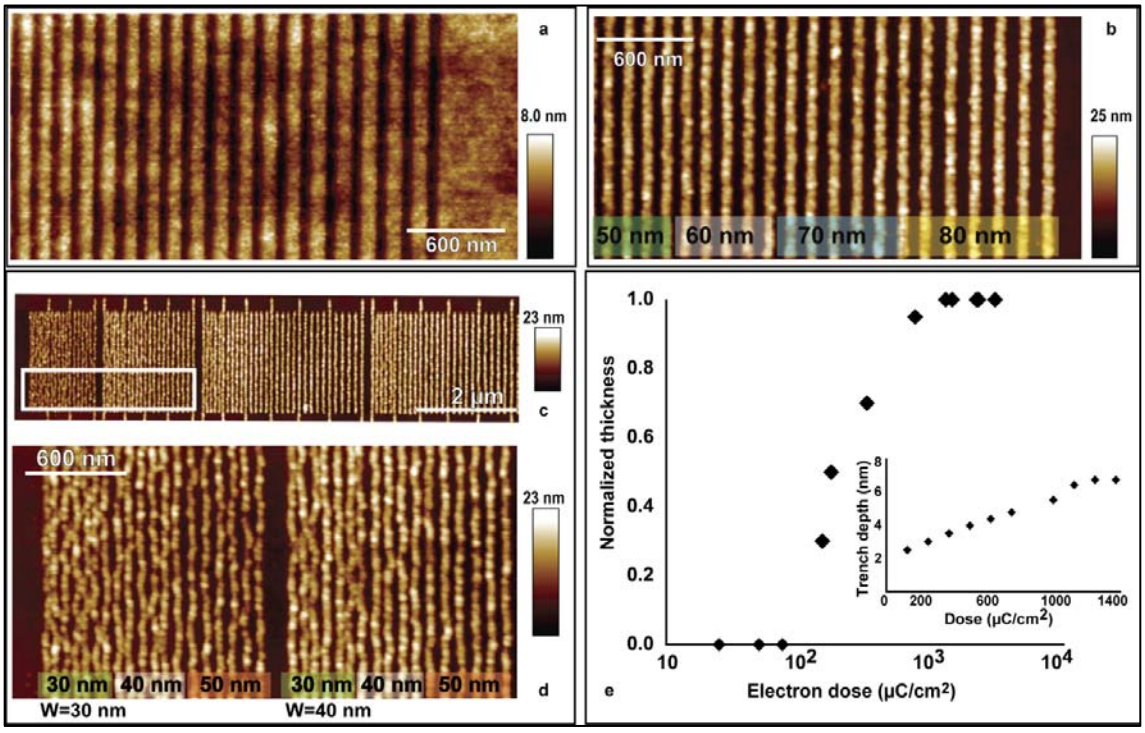

Figure 4-7 a) Atomic force microscopy (AFM) image before development, showing an e-beam exposed line array (line width 70 nm), **b)** AFM image after development of the structure shown in (a). The colored fields at the bottom indicate the pitch. **c)** AFM image of an array of lines exposed to 350 µC/cm^2 of e-beam radiation, **d)** an enlarged image showing lines with 30 and 40 nm in width and different distances, **e)** The sensitivity curve of Teflon AF, **inset)** Response of the Teflon AF film directly after exposure.

Considering the finding that overdevelopment does not occur, the lower solubility of e-beam exposed TAF in FC 75 might be associated with the formation of carboxyl groups, and the associated increase in hydrophilicity. More specifically, the degradation of TAF at the dioxole groups[120-121] decreases the FFV in the exposed areas, which, possibly along with the resulted higher density, reduces the solubility by restriction of solvent penetration into the polymer chains.

Since the exposed areas remain on the substrate after development, TAF can be considered as a negative e-beam resist. Using the contrast curve (Figure 4-7e), the sensitivity of TAF, i.e., the minimum energy required to define the structure after development, is ~175 μC/cm^2, and its contrast is calculated as $\gamma = (\log\frac{D_1}{D_0})^{-1} = 1.2.$, where D_1 is the dose at which the resist thickness does not change, and D_0 the dose at which the film is removed completely. The smallest feature size obtained by applying optimal conditions is 30 nm, determined in wide dense arrays of nanolanes with 40 nm pitch (Figure 4-7d). There are a number of factors that affect the resolution of the lithographic process, including initial film thickness, applied acceleration voltage, and development time and temperature. Accordingly, TAF is comparable with other common e-beam resists like HSQ (Hydrogen silsesquioxane) at the same acceleration voltage; (20 nm in width and pitches using 7000 μC/cm^2 on 50 nm-thick films).[122-123]

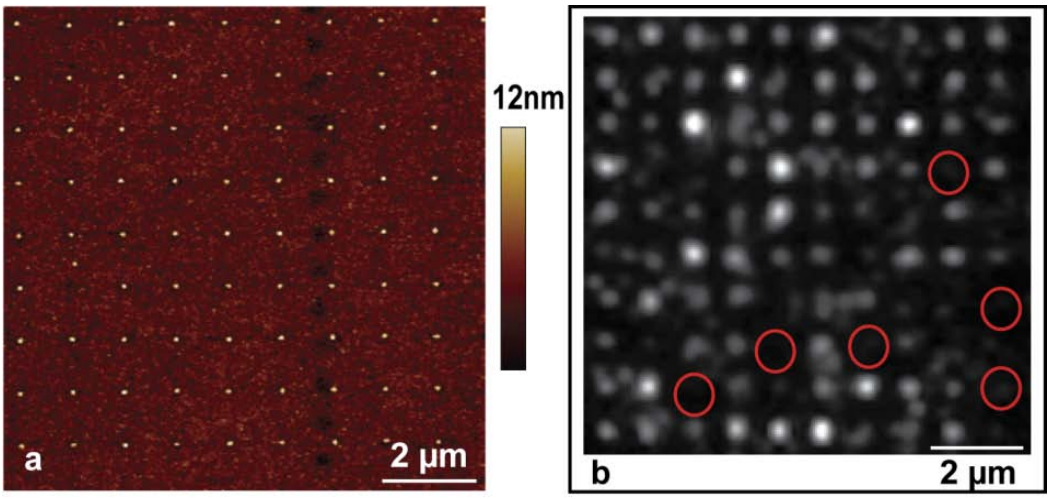

Figure 4-8 a) AFM micrograph of the surface after e-beam exposure and development of a 35 nm Teflon AF film. **b)** Total internal reflection fluorescence (TIRF) micrograph showing surface coverage after deposition of porphyrin/label-modified DNA assemblies.

One of the exemplary applications of TAF as an e-beam resist is shown in this thesis (paper III) where the interaction of DNA origami (cf. method section) with developed TAF was investigated. In this study, the rectangular DNA origamis modified with adhesion promoter anchors and fluorophores were deposited onto a glass surface patterned with an array of nanopillars of TAF with the same size as DNA origami (70×110 nm) and pitches of 1µm (Figure 4-8a).Using high resolution TIRF microscopy, it has been shown that developed TAF nanostructures selectively attract and accommodate DNA origamis with considerable surface coverage (Figure 4-8b).

The work on Teflon AF thin films revealed several interesting aspects, which can be developed into new applications. Sensing devices, optical components, and optimized cell culture surfaces are some of the possibilities this line of research offers.

5. METHODS

5.1. SUBSTRATE PREPARATION

The fabrication of customized micro/nano patterned surfaces using top-down nanotechnology approaches was an essential part of this thesis. All the fabrication and characterization steps have been performed in the clean-room environment at the Nanofabrication Laboratory MC2 at Chalmers. A brief introduction of photo- and electron beam lithography techniques is presented in the following section.

5.1.1. PHOTOLITHOGRAPHY

One of the approaches to generate microscale features on a surface is conventional photolithography, which is an optical printing process. Generally, this method comprises a sequence of processing steps, which differs slightly depending on the photoresist used, the nature of the substrate and other factors. Common process steps are:

- Pattern design and mask fabrication
- Preparation of the substrate including cleaning and deposition of a thin layer of a resist
- Soft baking of the resist
- Pattern exposure
- Image development

An example of the process is schematically depicted below (Figure 5-1):

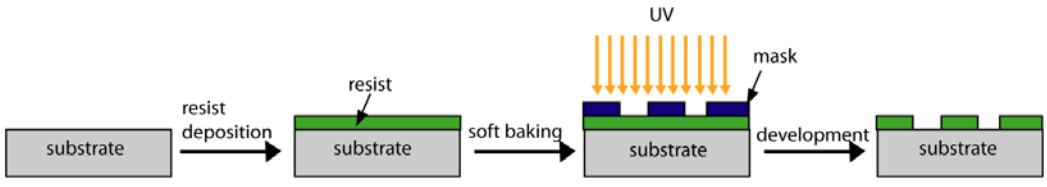

Figure 5-1 Essential steps in photolithography. The resist is positive, only the exposed areas are removed by the developer solution.

The mask is a chromium-coated glass or quartz plate, onto which the pattern has been transferred (e.g. by e-beam lithography), defining transparent and opaque regions. The pattern is commonly designed by 2D CAD software. To coat the substrate with a thin layer of a photosensitive polymeric material, i.e., photoresist, the spin-coating technique is typically used. After a baking step, which removes the solvent from the polymer film, substrate and mask are brought into close contact, and exposed to UV-A light for a defined time. The solubility of the exposed resist in the subsequently applied developer solution changes at this stage. If the solubility of the resist in the developer increases after exposure, the resist is referred to as "positive". This can be due to chain scission of the polymer, which increases its solubility directly or it can be because of the photolysis of a solubility-reducing additive in absence of which the polymer would be well soluble in the developer solution. In the case of "negative" photo resists, the solubility of the exposed regions decreases, caused by cross-linking of the resist's polymer chains, which is initiated by an added photoactive compound. The resolution of a photolithographic process is limited to a few micrometers due to scattering of light at longer wavelength. The resolution also depends on the type of photoresist, its thickness, and the exposure time. To complete the procedure, a chemical "developer" is used to selectively remove the more soluble part of the resist coating and thereby discriminates between the exposed and unexposed areas of the resist.[124]

In paper IV, photolithography is applied to fabricate microstructures on SU-8 substrates with a minimum feature size of approximately 1 μm. SU-8 is a negative tone resist, composed of bisphenol A Novolac epoxy dissolved in cyclohexanone or γ-butyrolactone, which is sensitive to UV-A light (360 nm). The photoactive catalytic additive of SU-8, triarylsulfonium hexafluoroantimonte, promotes the release of H^+ that consequently opens the epoxy rings in the side chains of the polymer (chemical amplification). The activated epoxy groups subsequently form covalent bonds with other epoxy groups on neighboring molecules and make effectively cross-linkined chains. SU-8 is a very common resist in microfabrication. It offers a high aspect ratio, high optical transparency, as well as good chemical stability and mechanical properties.[125]

5.1.2. ELECTRON BEAM LITHOGRAPHY (EBL)

Photolithography is not a suitable system for nanofabrication, due to the diffraction limit imposed by the comparatively long wavelength of the exposure light. By using deep UV lithography (λ~254 nm), the smallest achievable dimensions are of the order of 0.5-1 μm. One of the common approaches to overcome this limitation is using electron beam (e-beam) radiation instead of light. The history of electron beam lithography (EBL) goes back to the 1960s, when Mollenstedt and Speidel reported on the fabrication of high resolution patterns using a conventional scanning electron microscopy system.[126] Being a key to advancements in integrated circuit fabrication in the semiconductor industries, EBL systems have been developed remarkably in the past decades.[127] The fundamental procedure of EBL is in principle the same as in photolithography, comprising the designing of patterns, preparation of the substrate, pattern exposure, and development. The resist here is an electron beam sensitive material, and the substrate should be electrically conductive to avoid charging effects caused by the accumulation of electrons in the resist layer. E-beam resists are also grouped as positive and negative. An EBL system generally includes an electron gun to generate the beam, electron "optics" to adjust and deflect it, and also a calibrated stage control unit which enables the exposure in precisely defined locations on a large area of the substrate (Figure 5-2). In contrast to photolithography, which can be performed under ambient conditions, the whole procedure of EBL requires high vacuum.

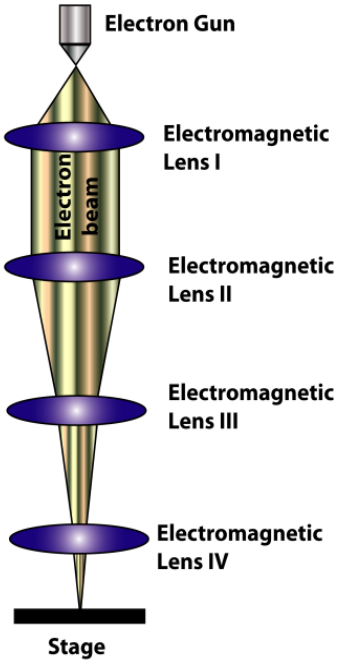

Figure 5-2 Simplified scheme of an electron beam lithography system. The electron radiation is accelerated at lens 1, and concentrated at lens 2. Lenses 3 and 4 are responsible for the deflection and focusing of the beam, respectively

The pattern for EBL is designed by means of CAD software, converted and transferred to the electron beam lithography system. The pattern is directly written onto the resist-coated substrate, which is subsequently developed in a suitable developer.

There are various influential phenomena occurring upon collision of the e-beam with the material (cf. scanning electron microscopy), among which scattering has the greatest impact. Depending on whether the electrons lose their energy partly or not, scattered electrons can be categorized as inelastic and elastic. The inelastic scattering, which deposits energy in the resist, is the main reason for pattern generation. Elastic scattering on the other hand, generates secondary electrons (SE), which have a negative effect on the resolution of lithographic process. Forward scattered electrons, with characteristic scattering angles < 90 degrees, travel short distances and tend to intensify the effect of the primary beam, which in turn broaden the size of the features. This effect can be diminished by applying thinner resist layers, or higher acceleration voltage. High energy backscattered electrons (BSE), on the other hand, travel longer distances, thereby reaching the substrate underneath the resist. BSE contribute to the proximity effect, i.e., an increased dose that a feature receives, that eventually results in uneven feature width of the pattern, and overexposure. Since the backscattering intensity has a reciprocal relation to the applied energy, higher acceleration voltage can reduce the proximity effect. Dose variation along the pattern is a useful technique to control the proximity effect, which has been used in the exposure of the lipid spreading lanes described in paper 1.[128-130]

E-beam lithography was used extensively in the work described in this thesis. In paper III, Teflon AF is introduced as a new negative non-amplified e-beam resist. In paper I and II, direct EBL is used to pattern Teflon AF surfaces, onto which cells and lipid monolayers have been patterned, and subsequently manipulated. The direct use of undeveloped patterns is a less common application of e-beam lithography-generated surfaces. The formation of recessed structures resulted from the degradation of Teflon AF during exposure, is exploited in paper I for confinement of lipid films, while the formation of new chemical moieties on the polymer substrate is promoting cell adhesion (paper II).

5.2. IMAGING TECHNIQUES

Obtaining highly resolved images of the fabricated micro- and nanoscale structures and devices was an important procedure in this thesis work, for which different variety of optical and non-optical microscopy techniques have been applied. The techniques were selected based upon the requirements and properties of the system under study, and the specific benefits that each of these techniques provides.

In paper II, bright-field microscopy was applied to image surface-adhered biological cells, while in papers I, III and IV, different fluorescence microscopy techniques were used to investigate the lipid film propagation, DNA origami localization and nano-tube formation, all of which cannot be visualized using conventional light microscopy, due to their optical properties. The non-optical imaging techniques have also been used to characterize the patterned surfaces. The techniques are described in more detail in the following sections.

5.2.1. OPTICAL MICROSCOPY TECHNIQUES

Since the invention of first practical microscope by van Leuwenhoek (1630s),[131] research to overcome the resolution limit, which arises from the diffraction barrier in optics, has led to various improvements and new imaging techniques. Generally, if the lateral distance between two points (r) in a sample is less than half of the wavelength of the used light, it cannot be resolved using a conventional light microscope. This is due to the constructive and destructive interferences between the diffraction originated Airy patterns of each point in the sample.[132] This can be quantified using the Rayleigh criterion (Equation 5-1).

$$r = \frac{0.61\lambda}{N.A.} \qquad \text{Eq.5-1}$$

where λ is the wavelength of the light, and NA is the numerical aperture of the microscope objective. The NA describes the capacity of the objective to collect as much

diffracted light as possible. It is linearly related to the refractive index (n) of the medium between the objective and the sample, as well as to the half-angle θ of the largest cone of light that can enter or exit the objective lens (Equation 5-2).

$$NA = n \sin \theta \qquad \text{Eq. 5-2}$$

Possibilities to increase the resolution (reducing r in eq. 5-1) include increasing the NA of the objective, either by means of sophisticated optics with a wider acceptance cone, or by increasing the refractive index of the medium between objective and sample. Another alternative to increase the resolution is the application of shorter wavelength light. The latter however, is not a favorable solution for studying biological samples, which can be degraded by short-wavelength (high energy) radiation.[133]

One way to increase the contrast of the image from transparent, unstained samples is by using diffraction interference contrast (DIC) microscopy. In this setup, a Nomarski prism is used before the sample, to split the light into two parallel, perpendicularly polarized rays. These rays pass through the sample in two adjacent points; therefore they diffract differently, which results in a relative phase shift. Another Nomarski prism after the sample recombines the two separated semi-coherent rays, where their interference results in different brightness of the image in different points, hence generating enhanced contrast.[134]

5.2.1.1. FLUORESCENCE MICROSCOPY

By using fluorescent probes in combination with one of several existing fluorescence-based microscopy imaging techniques, it is possible to study rather conveniently different aspects in optically transparent biological samples, including lipid monolayers, and lipid nanotubes. Position and distribution of the fluorophores in the sample, as well as fluorescence lifetime and interaction (energy transfer) are some examples of information that can be obtained by applying this technique.

In fluorescence microscopy, a light source excites a fluorescent species in the sample of interest. This species emits light of a longer wavelength, which produces the image

instead of the original excitation light. The fluorescent species (fluorophore, or fluorescent probe), is a chemical compound that re-emits light upon illumination with high efficiency.

When a photon interacts with a molecule, an electronic transition from the electronic ground state (E_0) to an excited state (E_n) can occur if the photon energy is of the order of E_{Ph}~(E_n-E_0). Subsequently, release of a photon is one of several different pathways to liberate the acquired energy of the photo-excited molecule. When a singlet electron in an excited state is paired with the electron in the ground state, the return of the electron to the ground state is allowed. The result is the emission of a photon (fluorescence), which possesses less energy in comparison with the absorbed photon, due to some loss that occurs by vibrational relaxation in the excited state.

The energy difference between absorbed and emitted photon (Stokes shift) mostly depends on the nature of the absorbing molecule. A number of other possible relaxation pathways, which are schematically expressed by the Jablonski diagram (Figure 5-3), are possible.[135]

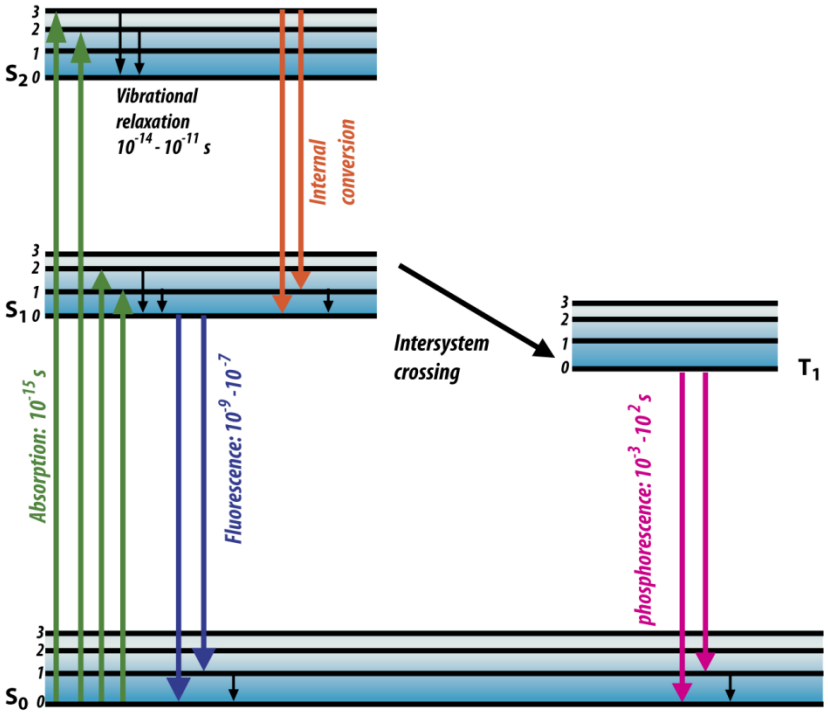

Figure 5-3 Jablonski diagram showing ground (S_0) and different excited states ($S_{1,2}$) as well as possible relaxation pathways

Fluorescence microscopy is based on separation of absorbed and emitted light, exploiting the Stoke shift. In this thesis three different fluorescence microscopy systems have been used, namely, wide-field fluorescence, total internal reflection, and confocal microscopy.

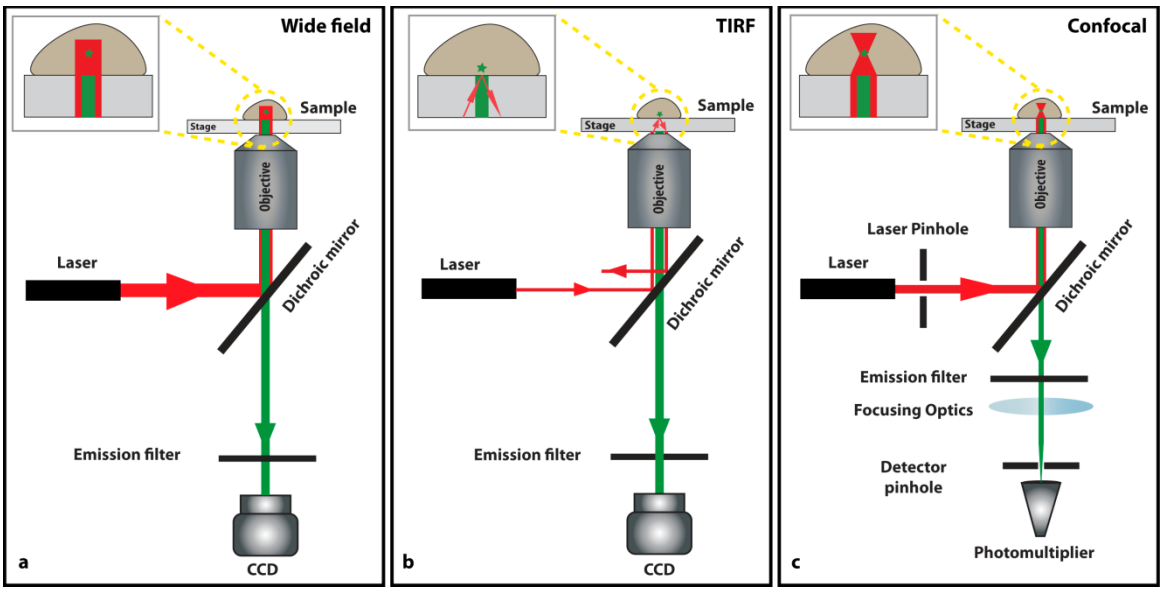

Figure 5-4 Simple schematic of fluorescence microscopy configurations. **a)** Wide-field laser induced fluorescence microscope, **b)** Total internal refraction microscope, and **c)** Confocal microscope

Laser-induced fluorescence microscopy (LIFM) is a wide-field technique, where a fluorophore-labeled sample is excited by a strong monochromatic light source, most commonly a laser beam. The exceptional intensity of the laser light improves the efficiency of the imaging by a higher rate of excitation. Moreover, the inherent monochromatic character of laser removes the need of application of excitation filters. Collecting of the emission light is done by the objective lenses, after which it is transferred to a camera (Figure 5-4 a). One of the main features in this microscopy setup is the use of a beam splitter in the light path before the objective, which separates emission and excitation light.

Total internal reflection microscopy (TIRF) is similar to LIFM, except that only a thin layer above the substrate surface is excited (Figure 5-4b). In this setup the excitation light is aligned in a way that the incident light is completely reflected at the interface of the sample and the medium. The resulted near-field wave, however, can travel a short distance through the sample and will therefore illuminate only the fluorophores that are in close vicinity of the interface. This in turn increases the quality of the obtained image extensively by eliminating the excitation of fluorophores in other parts of the sample. Improvements in resolution can be further achieved by super resolution microscopy techniques.

As an improved fluorescence-based method by **confocal microscopy**, even 3D-scanning of the sample is possible. Compared to the conventional optical microscope, wherein the entire sample is illuminated by the incident light, in a confocal microscopy system the emission light of only a specific horizontal plane (slice) of the sample at the focal point is collected (Figure 5-4c). The main beneficial feature of the confocal microscopy is that out-of-focal plane light, i.e., from above and below the focal point, is being removed by an aperture (pinhole) in front of the detector. Compared to wide field LIFM the resulting image is better defined.

Despite of the high selectivity and contrast, standard fluorescence microscopy techniques are still subject to the diffraction limit. This can be overcome by means of **super resolution microscopy** techniques like STORM, stochastic optical reconstruction microscopy. Relying on the Gaussian profile of the Airy disc from a single emitter, in STORM, the distances are extracted by mathematical analysis on the accumulated data obtained from a single point in a defined time window.[136] This essentially involves using photoswitchable fluorophores, i.e., fluorophores that goes through several dark and bright states before becoming bleached completely, to avoid overlapping of different points.[137] In paper III, STORM analysis was used to characterize the position of DNA origami on the Teflon AF nanopillars, where the fluorescence data were initially collected in the TIRF set-up.

5.2.2. NON-OPTICAL MICROSCOPY TECHNIQUES

Suffering from the diffraction limit, optical microscopy is unable to reveal finer details in the nanoscale. Moreover, optically transparent substrates are a requirement for most optical microscopy methods. As mentioned earlier in the lithography section, electron beam methods are one way to greatly improve resolution, where transparency is not a requirement. The advancement of nanotechnology is significantly indebted to the invention of scanning probe and scanning electron microscopy (SPM/SEM) techniques. In SPM, the interactions between the surface and a physical probe in a close proximity are measured, and the information is used to adjust the distance between probe and surface, while the probe is translated to scan the substrate. Examples of interactions are force, electrical current, surface potential, and magnetic force, each of which is the origin of different SPM technique. SEM employs an electron beam to scan the surface of a substrate, where secondary and/or backscattered electrons are collected to generate an image.

In paper I, III and IV atomic force microscopy (AFM) was used to characterize the patterned Teflon AF and Aluminum oxide surfaces, respectively. Moreover, to determine the surface potential of exposed Teflon AF, in paper I, Kelvin probe force microscopy (KPFM) was applied. Scanning electron microscopy (SEM) was used to image the patterned SU-8 surfaces in paper IV.

5.2.2.1. *ATOMIC FORCE MICROSCOPY (AFM)*

Atomic force microscopy (AFM), which was introduced in the 1980s, is one of the most powerful imaging techniques to characterize surfaces on nanometer length scales with sub-nanometer height resolution.[138]

In its most basic form, an AFM consists of five main elements.[139] A probe featuring a sharp tip with nanoscale curvature is attached to a flexible microcantilever. When the probe and the surface are brought into close proximity, different intermolecular interactions, like van der Waals and electrostatic forces, act in between them, causing a

deflection in the cantilever. The second element is a sensing system to detect the deflection. This is done usually by deflecting a laser beam off the cantilever towards a photodiode which is connected to a computer-operated feedback loop that keeps control of the position of the tip above the surface. A mechanical translation system for raster scanning of the sample, which is a piezoelectric actuator, and a monitoring component to convert the collected data into an image are the other essential components of the system (Figure 5-5).

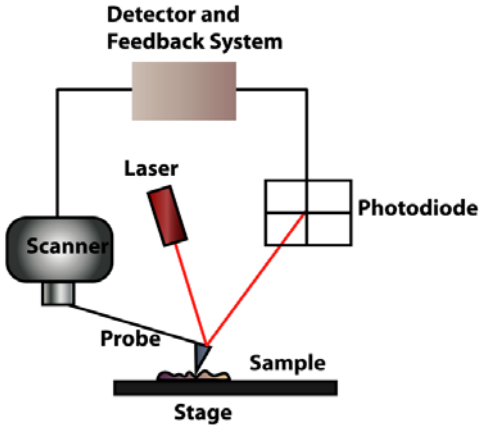

Figure 5-5 Schematic representation of atomic force microscopy set-up in contact mode. The deflection of the cantilever is determined by measuring laser beam displacement on a photodiode

Depending on the sample and desired information, AFM can be operated in one of three modes: contact, tapping, and non-contact. Affected by long-range intermolecular forces, the tapping mode image is formed by the change in oscillation amplitude or phase of a cantilever operating close to its resonance frequency. This is a preferred mode to scan soft matter, due to the mild, non-destructive operation conditions.[140] The resolution of AFM greatly depends on factors such as the quality of tip, optimum scan rate, and the use of a tip with a proper spring constant. Coating and sharpness also affect extensively the resolution of final image. Since its invention, AFM went through considerable technological developments by which the properties of the sample other than its topography can be studied. Relying on different interactions between probe and sample mechanical,[141] magnetic,[142] and electrical measurements[143] for instances are possible by AFM, using customized tips and setups.

5.2.2.2. KELVIN PROBE FORCE MICROSCOPY (KPFM)

Kelvin probe force microscopy (KPFM) was first introduced by Nonnenmacher in 1991 as a new AFM setup to measure the local surface potential with nanometer lateral resolution.[144] With respect to setup and operation, this instrumental technique is quite

similar to AFM. The cantilever in KPFM, however, must be conductive, which is typically achieved by using highly doped semiconductor, or metallized ordinary AFM cantilevers.[145]

KPFM measures the work function (Φ) difference between the sample surface and the tip. When the probe and the surface are close enough to each other, there is an electrical force between them due to the difference in their Fermi energies. Upon connecting tip and sample with an electric circuit (measurement setup), the initial electron flow equilibrates the Fermi energy levels, and accumulates charges on the tip and the surface, which generates an external voltage difference (contact potential difference, CPD). By applying a DC voltage with the same magnitude in opposite direction through the measurement setup, the surface charge is diminished by an amount which equals the voltage difference between the tip and the sample, allowing the surface potential to be quantified (Figure 5-6). Obtaining a high resolution KPFM image is greatly dependent on the sharpness and conductivity of the probe, as well as on the conductivity between the cantilever and the probe holder. Owing to the non-destructive nature of the method, the application of KPFM to study the electrical properties of biological samples and polymers is growing extensively. In paper I, KPFM was used to determine the difference in surface potential between exposed and unexposed Teflon AF.

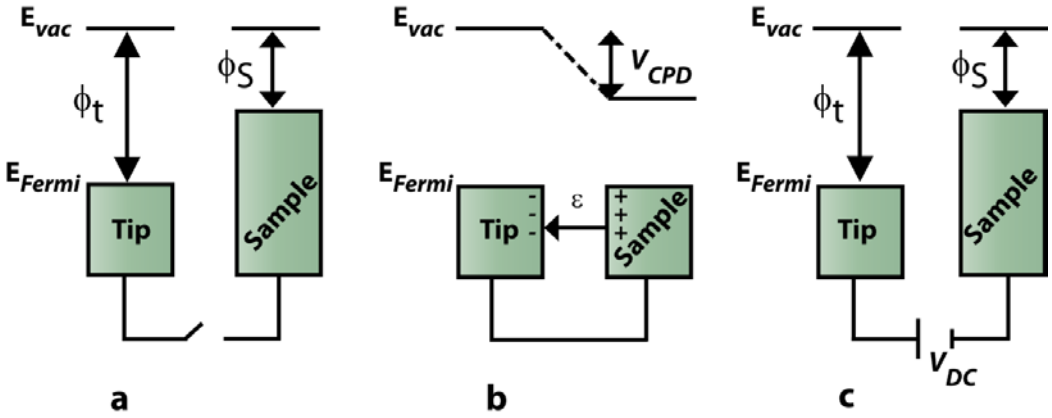

Figure 5-6 Fermi energy levels. **a)** The tip and sample are close but not electrically connected, **b)** Fermi levels align when the tip and sample are electrically connected, **c)** The electrostatic field is canceled by applying external voltage in opposite direction.

5.2.2.3. SCANNING ELECTRON MICROSCOPY (SEM)

The scanning electron microscope (SEM) is undoubtedly one of the most influential instruments in modern physics and material science. It helped extensively to initiate the nanotechnology revolution by providing the possibility to directly observe the nanoscale features. After three decades of developments following the demonstration of the SEM principle by von Ardenne in 1937, the first commercial SEM was introduced in 1965 by the Cambridge Scientific Instrument Company.[146] Nowadays the SEM is a particularly versatile instrument that is widely used both in industry and academic research laboratories in many different fields to characterize the materials.

Constituting actually the origin of electron beam lithography, the main instrumental concept and structure of SEM is very similar to EBL. In contrast to EBL, however, the beam in a SEM system is used to image the sample rather than causing structural changes in a resist film. The SEM is composed of an electron column to generate and control the beam, a chamber to provide vacuum, hold and manipulate the sample, different detectors to collect the signals, and finally a computer to generate the image. As mentioned earlier in e-beam lithography section, when the primary electrons of the beam (PE) reach the surface of a material, they can be scattered slightly (forward scattering) or heavily (backscattering). Moreover, upon the collision of high energy PE, different type of electron transitions in the material can occur, which generate secondary electrons (SE), i.e., the released valence electrons from surface atoms, also Auger electrons or x-ray radiation during the associated relaxation processes (Figure 5-7).

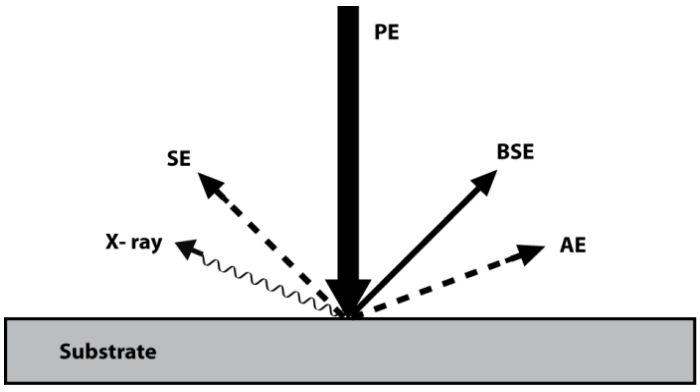

Figure 5-7 Simplified illustration of electron beam interaction with solid material

Detection of secondary electrons (SE) by means of the Everhart-Thornley detector is the most common SEM mode to create a surface topography image.[146] This detector consists of a scintillator that emits luminescence photons when being excited by SEs, and a photomultiplier that converts photons to intensified electrons.

Even though the secondary electrons can be ejected from all the atoms of the material, only the ones from the surface will produce a detectable signal. The rest usually gets reabsorbed before reaching the surface. Therefore, back scattered electrons (BSE) are collected by a solid state BSE detector, and are used to obtain information about deeper regions of the sample, by providing higher contrast based on the average atomic number of the material in the sample.[147] The X-ray signal provides detailed information about the composition of the material. This is of particular importance when working with unknown samples. Accordingly, modern SEMs are equipped with an energy dispersive x-ray detector as well.[148]

In paper IV, SEM was used to characterize the micro-scale SU-8 photoresist lanes on a Ti/Al-coated glass substrate (Figure 5-8), which was designed to confine and direct lipid double bilayer patches after displacing them by means of an infrared beam.

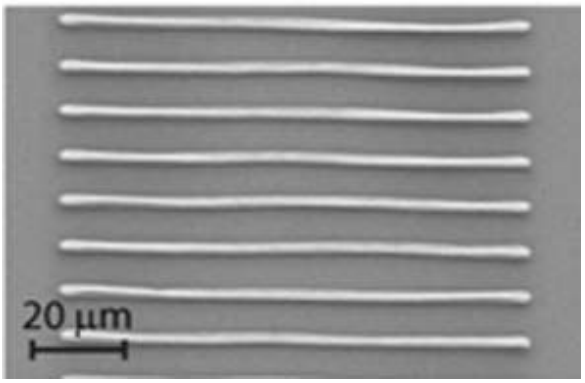

Figure 5-8 Scanning electron micrograph (SEM) of the photolithographically generated SU-8 lanes (metallized) on a glass substrate

5.3. OTHER METHODS

5.3.1. DNA ORIGAMI

One of the interesting examples of organized structures in biological cells is Deoxyribonucleic acid (DNA), a natural macromolecular assembly that carries all the biological information of living organisms. Discovered by Watson, Crick and Franklin in the 1950s, DNA is a twisted double-strand copolymer of sugar, branched with adenine (A), guanine (G), cytosine (C) and thymine (T) (Figure 5-9a).[149] The special ability to form hydrogen bonds in between complementary nucleotide bases is not only the key to the helix structure of DNA (Figure 5-9b), which in turn is responsible for the rigidity and stability of the molecule, but it also enables DNA to carry biological information encoded in different base sequences.

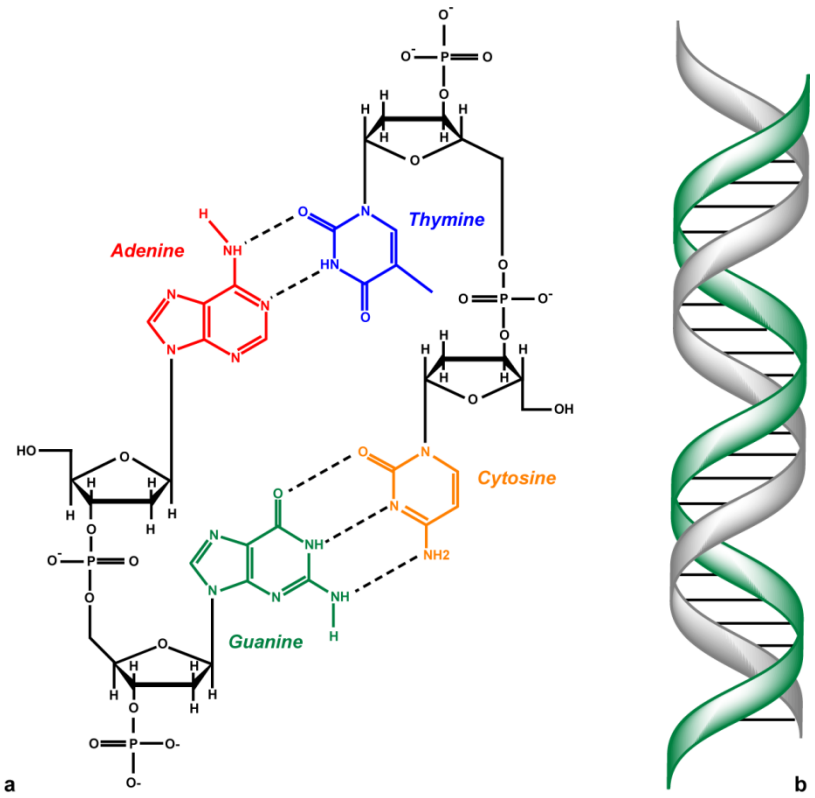

Figure 5-9 a) Four DNA nucleobases connected to sugar backbone and paired by hydrogen bonds (dashed lines), **b)** Schematic representation of DNA helix

The latter has inspired applications of DNA as a programmable device in non-biological contexts. Structural DNA nanotechnology, introduced by Seeman in late 1980s, focuses on the technological applications of engineered DNA building blocks as scaffolds,[150]

delivery of cargo,[151] molecular switches,[152] and computing devices[153], in all of which the self-assembly feature of DNA (a bottom-up approach) is essential.[154]

One of the advanced examples of self-assembled DNA technology is the DNA origami device concept, which involves a long, single DNA strand folded to a pre-designed shape by using shorter strands or "staples" as "smart" glue (Figure 5-10a). The geometry of the final structure can be widely varied depending on the staple sequence.[155] In comparison with other DNA-based materials,[156] DNA origami provides the opportunity to synthesize functional nanoscale scaffolds by chemical functionalization of selected staples.[157] Table 5-1 shows examples of modified staple strands used in paper III. This opens opportunities for designing devices for application in biosensing or light-harvesting.[158-159]

Table 5-1 Staple strand modifications

Strand	Sequence	Modification
1	TAGATGGGGGGTAACGCCAGGGTTGTGCCAAG*	ATTO-647N
2	CTTGCATGCATTAATGAAT*CGGCCCGCCAGGG	Porphyrin
3	TTTGCCAGATCAGTTGAGATTTAGTGGTTTAA*	ATTO-647N
4	TTTCAACTATAGGCTGGCT*GACCTTGTATCAT	Porphyrin

** shows the position of a modification, for example: T* means that this thymine base is modified.*

In the paper, the nanopatterned Teflon AF is used to accommodate single DNA origami structures in pre-designed positions with high spatial precision, where hydrophobic porphyrin groups in the origami were used to promote its adhesion to the substrate (Figure 5-10b).

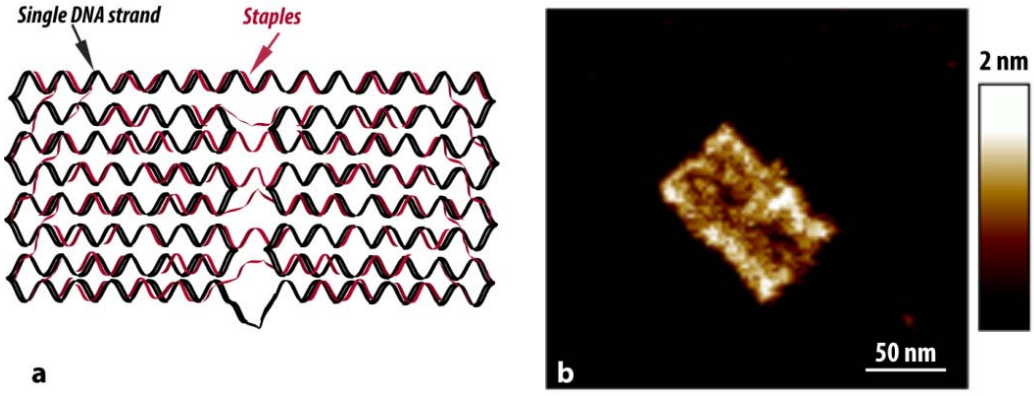

Figure 5-10 a) Schematic representation of rectangular DNA origami, **b)** Atomic Force microscopy image of DNA origami on mica

5.3.2. CELL CULTURING

In paper II, the interaction of cells with e-beam patterned Teflon AF surfaces has been investigated. Adherent Chinese hamster ovary (CHO), Human embryonic kidney (HEK293), and Human neuroblastoma (SH-SY5Y) are three different embryonic cell lines that have been used in this study. All cells have been cultivated in their respective medium (Table 5-2) at 37° C in a humidified 5% CO_2 atmosphere. Cell handling was performed under standard conditions,[160] using sterilized equipments in a laminar flow hood, at dedicated cell facilities. The procedures for culturing and cell transfer are described in detail in paper II.

Table 5-2 Culturing medium used for different cell lines

Cell Line	Culturing medium
CHO	Dulbecco's modified eagle medium (DMEM), 2mM L-glutamine, 10% of fetal bovin serum (FBS), 350 μgmL^{-1} of zeocin, 5$\mu g\ mL^{-1}$ of blasticidin
HEK 293	DMEM, 2mM L-glutamine, 10% FBS
SH-SY5Y	modified Eagle's medium (MEM), 2mM L-glutamine, 10% FBS, 1% of non-essential amino acids, Ham's F12

6. SUMMARY & REMARKS

This work reported on new approaches to the fabrication of soft matter nanodevices, with a special focus on patterning and manipulation of lipid monolayers, cells and DNA origami.

In paper I, direct electron beam lithography was used to fabricate nanostructures on Teflon AF surfaces suitable for confining and patterning lipid monolayers. E-beam exposure causes chemical changes in the fluorinated polymer structure, changing the surface properties such that self-spreading can no longer be observed. This was exploited to "draw" a frame around a selected region on a Teflon AF surface, which efficiently confines a spreading lipid film within its boundaries. The lipid material, fluorescently labeled with Texas Red and ATTO 488, were manually deposited on the patterned surface. Confocal microscopy was then applied to follow the spreading process, and investigate the propagation of the lipid film in nanosized constrictions. Characteristic chemical and physical properties of the Teflon AF surface were investigated by means of AFM, XPS, WAC and KPFM. By optimization of pattern geometry and radiation dose the propagating lipid film could be guided through nanolanes as narrow as 50 nm. The frame-patterning technique represents a new surface preparation strategy for the controlled formation of self-assembled molecularly thin lipid films. It can possibly be developed into a versatile research platform for 2D chemical reactions and single molecule studies, combining superior optical properties with minimal fabrication effort.

In paper II, a new method was introduced for defining patterns of adhered biological cells on Teflon AF surfaces. It is shown that the e-beam exposed Teflon AF surfaces support the adhesion of different immortalized embryonic cell lines (HEK293, CHO and SH-SY5Y), in which the geometry of the irradiated pattern is a key element which affects the adhesion of the cells. By taking advantage of the structural differences between unexposed and e-beam-exposed surface areas, which are reflected in their cytophilicity, the need of adhesion promoting biomolecules is effectively eliminated. For example, neat and well-defined networks of neurons (SH-SY5Y) have been fabricated. The method is

the foundation for rapid cell pattern generation under non-contaminating conditions, which is one of the necessities for advanced studies in cell-to-cell communication, cell migration and other dynamic phenomena related to the proliferation of biological cells.

In paper III, Teflon AF was further developed into a negative e-beam resist. By applying the perfluorinated organic solvent 2-butyl tetrahydrofurane (FC 75) as developing solvent on e-beam patterned Teflon AF surfaces, dense arrays of nanolanes with a feature size as small as 30 nm in width and 40 nm in pitch have been consistently obtained. The sensitivity of the resist has been calculated as ~175 μC/cm^2 with the resist contrast of γ = 1.2. In an application example it has been shown that the developed nanostructure pillars of Teflon AF can be used to site-selectively accommodate rectangular single DNA origami units with a surface coverage > 80%. Hydrophobic porphyrin anchors were used to promote the deposition of the DNA origami structures on the Teflon AF nanopillars. The nanopillars were characterized by AFM and the porphyrin/DNA origami by dSTORM super-resolution microscopy. This exemplary application of Teflon AF as e-beam resist shows that novel combinations of various biological and synthetic materials are possible on the nanoscale, which has potential for advanced applications in, e.g., biosensing and 2D chemical reactor design.

In paper IV, a contact-free soft matter fabrication technology to generate networks of lipid nanotubes and flat giant unilamellar vesicles was introduced. For this unconventional fabrication method, a lipid double bilayer patch on a transparent alumina-coated glass substrate was locally exposed to a focused IR-B beam, causing migration of lipid material on the surface due to temperature-dependent local adhesion differences between lipid film and surface. Nanotubes were found to interconnect the separated lipid film patches, generating two-dimensional, truly nanofluidic flat giant-vesicle-nanotube networks. In the paper, the thermomigration of lipid membrane was further directed through micro-sized lanes, which were photolithographically defined in SU-8, prior to Al_2O_3 deposition. Nanotubes of μm length were thus fabricated on-demand in desired locations without the need of point forces exerted by microneedles or beads.

Interdisciplinary research is one way to expand the boundaries of scientific exploration, and in the life sciences currently the most promising route to solutions to complex research problems, for example the need for fast and reliable diagnostics, or new biocompatible materials and information processing technologies. By combining state-of-the-art materials and technologies, new experimental opportunities are opened up to address fundamental research questions, and to solve practical problems in different application areas. In the work presented here, a number of specific problems have been tackled using micro- and nanotechnologies, new materials and biomimetic principles.

Future research directions based upon the scientific findings described herein, and in some cases even wider applications, can indeed be envisioned.

Many unknown aspects of lipid monolayer dynamics are remained unsolved that need to be addressed. Until now, very little is known about the front edge of a spreading monolayer, and the observed thinning effect. In this regard, the monolayer membrane device on the Teflon substrate can offer an adaptable platform to target such questions. There are also interesting physical phenomena, such as the 2D evaporation and the filter effect, observed during the experimental work, which require further exploration. Moreover, by knowing the optimum requirements to design a versatile device, a system can be fabricated in which several different lipid flows meet at a nano - intersection, where the kinetics and reaction dynamics can be investigated at the molecular scale, using high resolution techniques, in particular single molecule microscopy.

The new chemical-free cell culturing substrate, on the other hand, provides a unique platform onto which different aspects of cell-surface interaction as well as cell-cell communication can be controllably studied. Knowing that different cell lines require different geometries for successful adhesion, this kind of substrate could become valuable in tissue engineering. The substrate also has potential in neuroscience research, by offering a facile method to design and culture sophisticated neuronal networks of desired structure and function. To begin with, future investigations should be focused upon establishing the details of the cell-adhesion mechanism on the patterned area. The capability to promote and support the formation of nanotubes between cultured cells is

another distinctive feature of this substrate which may greatly facilitate cell-cell interaction studies.

Thematically closely connected, might be future studies on biomimetic nanotube - FGUV networks produced by thermomigration of membranes, which is a less complicated and better configurable alternative to investigating transport phenomena within nanotubes.

Last but not least, the development of a new, relatively simple Teflon AF nanopatterning technique might lead to various new technological applications. The possibility of simple functionalization of the patterned areas of Teflon AF, which feature chemically reactive carbonyl moieties, is an example. From bio-application point of view, Teflon AF as a negative e-beam resist clearly has benefits over other commercially available resists. Standardized processes for pattern generation, refined exposure strategies and other improvements would support wider use by life science researchers in the future. In this context, Teflon AF 2400 instead of Teflon AF 1600 is also an interesting material to be explored.

ACKNOWLEDGEMENTS

I express my deepest gratitude to the following people:

My supervisor, **Aldo Jesorka**, for believing in me and accepting me in your group. For your brilliant ideas and discussions, and for your endless support.

My co-supervisor, **Samuel Lara Avila**, who was always there helping me through difficult situations in the lab. Thank you for your precious advices and suggestions.

My co-supervisor, **Kent Jardemark,** for very helpful and interesting discussions.

My co-authors, for your invaluable contribution.

Patrik, **Jakob**, **Bo**, **Laura** and **Neserine**, for very interesting discussions and fantastic collaboration. It was a great opportunity exploring new research fileds with you!

Irep, Erik, Carolina, Dou Dou, Haijang, Patrik and **Emelie**, for sharing your lab experiences with me. I was so lucky having great coaches like you!

Gavin, for all the microscopy support and interesting discussions.

Samuel, **Hoda** and **Pegah**, for proof-reading this thesis.

All the process lab crew in MC2, especially **Bengt Nilsson**, for the technical assistance with the e-beam lithography system.

Alexei Kalaboukhov, for helping me with the KPFM.

Anne Wendel for XPS analysis.

The people at the physical chemistry division, especially the current and former members of the Biophysical Technology Lab, for such a pleasant work environment. I enjoyed every minute being at work because of you!

The best officemates in the world: **Ilona** and **Tanya**. It was a great fortune sharing my time with you. Thank you for creating a nice atmosphere, bearing me in bad moments and being such great support!

My wonderful friends, **Nina**, **Robert**, **Negin, Maryam**, **Celine**, **Hoda**, **Pegah** , **Jessica, Daniel** and **Tanya:** thank you for all the beautiful unforgettable moments.

My fantastic parents **Homa** & **Jafar** for your never-ending support and encouragement. I would not have made it this far without you.

And my best friend **Mazdak**, for your unconditional love, support and patience. Life is a joyful beautiful journey with you! Love you so much!

BIBLIOGRAPHY

1. Feynman, R.P., *There's plenty of room at the bottom (data storage).* Journal of Microelectromechanical Systems, **1992**. 1(1): p. 60-66.

2. Theis, T., Parr, D., Binks, P., Ying, J., Drexler, K.E., Schepers, E., Mullis, K., Bai, C.L., Boland, J.J., Langer, R., Dobson, P., Rao, C.N.R., and Ferrari, M., *Nan'o.Tech.Nol'o.Gy n.* Nature Nanotechnology, **2006**. 1(1): p. 8-10.

3. Binnig, G. and Rohrer, H., *Scanning tunneling microscopy.* Helvetica Physica Acta, **1982**. 55(6): p. 726-735.

4. Toumey, C., *Plenty of room, plenty of history.* Nature Nanotechnology, **2009**. 4(12): p. 783-784.

5. Schomburg, W., *Scaling laws*, in *Introduction to microsystem design*. **2011**, Springer Berlin Heidelberg. p. 3-4.

6. Drexler, K.E., *Productive nanosystems: The physics of molecular fabrication.* Physics Education, **2005**. 40(4): p. 339-346.

7. Koch, C.C., Books24x, Sciencedirect, and Knovel, *Nanostructured materials: Processing, properties, and applications.* Vol. 2nd; 2; 2. **2007**, Norwich, NY: William Andrew Pub.

8. Whitesides, G.M. and Grzybowski, B., *Self-assembly at all scales.* Science, **2002**. 295(5564): p. 2418-2421.

9. Ozin, G.A., Hou, K., Lotsch, B.V., Cademartiri, L., Puzzo, D.P., Scotognella, F., Ghadimi, A., and Thomson, J., *Nanofabrication by self-assembly.* Materials Today, **2009**. 12(5): p. 12-23.

10. Quéré, D., *Soft-matter miracles.* Nature, **2010**. 465(7301): p. 1011.

11. Richter, R.P., Berat, R., and Brisson, A.R., *Formation of solid-supported lipid bilayers: An integrated view.* Langmuir, **2006**. 22(8): p. 3497-3505.

12. Czolkos, I., Jesorka, A., and Orwar, O., *Molecular phospholipid films on solid supports.* Soft Matter, **2011**. 7(10): p. 4562-4576.

13. Elliott, J.T., Burden, D.L., Woodward, J.T., Sehgal, A., and Douglas, J.F., *Phospholipid monolayers supported on spun cast polystyrene films.* Langmuir, **2003**. 19(6): p. 2275-2283.

14. Shimizu, T., Masuda, M., and Minamikawa, H., *Supramolecular nanotube architectures based on amphiphilic molecules.* Chemical Reviews, **2005**. 105(4): p. 1401-1444.

15. Sanii, B. and Parikh, A.N., *Surface-energy dependent spreading of lipid monolayers and bilayers.* Soft Matter, **2007**. 3(8): p. 974-977.

16. Hu, X.C., Damjanovic, A., Ritz, T., and Schulten, K., *Architecture and mechanism of the light-harvesting apparatus of purple bacteria.* Proceedings of the National Academy of Sciences of the United States of America, **1998**. 95(11): p. 5935-5941.

17. Hu, X.C. and Schulten, K., *How nature harvests sunlight.* Physics Today, **1997**. 50(8): p. 28-34.

18. Katterle, M., Prokhorenko, V.I., Holzwarth, A.R., and Jesorka, A., *An artificial supramolecular photosynthetic unit.* Chemical Physics Letters, **2007**. 447(4-6): p. 284-288.

19. Wright, C.H.G. and Barrett, S.F., *Chapter 1 - biomimetic vision sensors*, in *Engineered biomimicry*, A. Lakhtakia and R.J. Martín-Palma, Editors. **2013**, Elsevier: Boston. p. 1-36.

20. Huang, J., Wang, X., and Wang, Z.L., *Bio-inspired fabrication of antireflection nanostructures by replicating fly eyes.* Nanotechnology, **2008**. 19(2): p. 025602.

21. Wang, X., Wang, M., Ding, B., and Yu, J., *Engineering biomimetic superhydrophobic surfaces of electrospun nanomaterials.* Nano Today, **2011**. 6(5): p. 510-530.

22. Ferrari, M., *Cancer nanotechnology: Opportunities and challenges.* Nature Reviews Cancer, **2005**. 5(3): p. 161-171.

23. Rösler, A., Vandermeulen, G.W.M., and Klok, H.-A., *Advanced drug delivery devices via self-assembly of amphiphilic block copolymers.* Advanced Drug Delivery Reviews, **2001**. 53(1): p. 95-108.

24. Staples, M., Daniel, K., Cima, M.J., and Langer, R., *Application of micro- and nano-electromechanical devices to drug delivery.* Pharmaceutical Research, **2006**. 23(5): p. 847-863.

25. Jain, K.K., *Nanomedicine: Application of nanobiotechnology in medical practice.* Medical Principles and Practice, **2008**. 17(2): p. 89-101.

26. Pehlivan, S.B., *Nanotechnology-based drug delivery systems for targeting, imaging and diagnosis of neurodegenerative diseases.* Pharmaceutical Research, **2013**. 30(10): p. 2499-2511.

27. Shuttleworth, R., *The surface tension of solids.* Proceedings of the Physical Society of London Section A, **1950**. 63(365): p. 444-457.

28. Indekeu, J., Bonn, D., Meunier, J., Rolley, E., and Eggers, J., *Wetting and spreading.* Reviews of Modern Physics, **2009**. 81(2): p. 739-805.

29. Wenzel, R.N., *Surface roughness and contact angle* Journal of Physical and Colloid Chemistry, **1949**. 53(9): p. 1466-1467.

30. Cassie, A.B.D. and Baxter, S., *Wettability of porous surfaces.* Transactions of the Faraday Society, **1944**. 40: p. 0546-0550.

31. Nychka, J.A. and Gentleman, M.M., *Implications of wettability in biological materials science.* JOM, **2010**. 62(7): p. 39-48.

32. Kallay, N., Preocanin, T., Kovacevic, D., Lützenkirchen, J., and Chibowski, E., *Electrostatic potentials at solid/liquid interfaces.* Croatica Chemica Acta, **2010**. 83(3): p. 357.

33. Fenderson, B., *Molecular biology of the cell,5th edition.* Medicine & Science in Sports & Exercise, **2008**. 40(9): p. 1709.

34. Wang, Z., Wang, Y., Cai, W.-J., and Liu, S.-Y., *A long pathlength spectrophotometric pco2 sensor using a gas-permeable liquid-core waveguide.* Talanta, **2002**. 57(1): p. 69-80.

35. Van Meer, G., Voelker, D.R., and Feigenson, G.W., *Membrane lipids: Where they are and how they behave.* Nature Reviews Molecular Cell Biology, **2008**. 9(2): p. 112-124.

36. Fenske, D.B., Monck, M.A., Cullis, P.R., and Hope, M.J., *The functional roles of lipids in biological membranes*, in *Biomembranes: A multi-volume treatise*, A.G. lee, Editor. **1995**, JAI. p. 1-28.

37. Gennis, R.B., Springerlink, and Springerlink, A., *Biomembranes: Molecular structure and function*. **1989**, New York, NY: Springer New York.

38. Israelachvili, J.N., *Intermolecular and surface forces*. 3rd ed. **2011**: Elsevier Inc.

39. Cullis, P.R. and Dekruijff, B., *Lipid polymorphism and the functional roles of lipids in biological membranes.* Biochimica Et Biophysica Acta, **1979**. 559(4): p. 399-420.

40. Krister Holmberg, B.J., Bengt Kronberg, Björn Lindman, *Surfactants and polymers in aqueous solution*. 2nd ed. **2002**: John Wiley & Sons, Ltd.

41. Mcconnell, H.M., Watts, T.H., Weis, R.M., and Brian, A.A., *Supported planar membranes in studies of cell-cell recognition in the immune system.* BBA - Reviews on Biomembranes, **1986**. 864(1): p. 95-106.

42. Tamm, L.K. and Mcconnell, H.M., *Supported phospholipid bilayers.* Biophysical Journal, **1985**. 47(1): p. 105-113.

43. Simonsson, L. and Hook, F., *Formation and diffusivity characterization of supported lipid bilayers with complex lipid compositions.* Langmuir, **2012**. 28(28): p. 10528-10533.

44. Baoukina, S. and Tieleman, D.P., *Lung surfactant protein sp-b promotes formation of bilayer reservoirs from monolayer and lipid transfer between the interface and subphase.* Biophysical Journal, **2011**. 100(7): p. 1678-1687.

45. Tanaka, M. and Sackmann, E., *Supported membranes as biofunctional interfaces and smart biosensor platforms.* Physica Status Solidi a-Applications and Materials Science, **2006**. 203(14): p. 3452-3462.

46. Castellana, E.T. and Cremer, P.S., *Solid supported lipid bilayers: From biophysical studies to sensor design.* Surface Science Reports, **2006**. 61(10): p. 429-444.

47. Dabkowska, A.P., Michanek, A., Jaeger, L., Rabe, M., Chworos, A., Hook, F., Nylander, T., and Sparr, E., *Assembly of rna nanostructures on supported lipid bilayers.* Nanoscale, **2015**. 7(2): p. 583-596.

48. Czolkos, I., Erkan, Y., Dommersnes, P., Jesorka, A., and Orwar, O., *Controlled formation and mixing of two-dimensional fluids.* Nano Letters, **2007**. 7(7): p. 1980-1984.

49. Im, H., Wittenberg, N.J., Lesuffleur, A., Lindquist, N.C., and Oh, S.H., *Membrane protein biosensing with plasmonic nanopore arrays and pore-spanning lipid membranes.* Chemical Science, **2010**. 1(6): p. 688-696.

50. Roberts, G.G., *Langmuir-blodgett films*. **1990**, New York: Plenum.

51. Reimhult, E., Kasemo, B., and Höök, F., *Rupture pathway of phosphatidylcholine liposomes on silicon dioxide.* **2009**(Journal Article).

52. Ainla, A., Gozen, I., Hakonen, B., and Jesorka, A., *Lab on a biomembrane: Rapid prototyping and manipulation of 2d fluidic lipid bilayers circuits.* Scientific Reports, **2013**. 3.

53. Hirtz, M., Oikonomou, A., Varey, S., Fuchs, H., and Vijayaraghavan, A., *Multiplexed biomimetic lipid membranes on graphene by dip-pen nanolithography.* Microscopy and Microanalysis, **2014**. 20(S3): p. 2058-2059.

54. Dommersnes, P.G., Orwar, O., Brochard-Wyart, F., and Joanny, J.F., *Marangoni transport in lipid nanotubes.* Europhysics Letters, **2005**. 70(2): p. 271-277.

55. Gennes, P.G.D., Brochard-Wyart, F., and Quéré, D., *Capillarity and wetting phenomena: Drops, bubbles, pearls, waves*. **2004**, New York: Springer.

56. Czolkos, I., *Micro- and nano-scale devices for controlling two-dimensional chemistry*. **2009**, Chalmers University of Technology, Sweden: Göteborg.

57. Ding, J.Q., Takamoto, D.Y., Von Nahmen, A., Lipp, M.M., Lee, K.Y.C., Waring, A.J., and Zasadzinski, J.A., *Effects of lung surfactant proteins, sp-b and sp-c, and palmitic acid on monolayer stability.* Biophysical Journal, **2001**. 80(5): p. 2262-2272.

58. Bron, A.J., Tiffany, J.M., Gouveia, S.M., Yokoi, N., and Voon, L.W., *Functional aspects of the tear film lipid layer*. Experimental Eye Research, **2004**. 78(3): p. 347-360.

59. Kulovesi, P., Telenius, J., Koivuniemi, A., Brezesinski, G., Rantamaki, A., Viitala, T., Puukilainen, E., Ritala, M., Wiedmer, S.K., Vattulainen, I., and Holopainen, J.M., *Molecular organization of the tear fluid lipid layer.* Biophysical Journal, **2010**. 99(8): p. 2559-2567.

60. Czolkos, I., Hakonen, B., Orwar, O., and Jesorka, A., *High-resolution micropatterned teflon af substrates for biocompatible nanofluidic devices.* Langmuir, **2012**. 28(6): p. 3200-3205.

61. Erkan, Y., Halma, K., Czolkos, I., Jesorka, A., Dommersnes, P., Kumar, R., Brown, T., and Orwar, O., *Controlled release of chol-teg-DNA from nano- and micropatterned su-8 surfaces by a spreading lipid film.* Nano Letters, **2008**. 8(1): p. 227-231.

62. Czolkos, I., Hannestad, J.K., Jesorka, A., Kumar, R., Brown, T., Albinsson, B., and Orwar, O., *Platform for controlled supramolecular nanoassembly. (vol 9, pg 2482, 2009).* Nano Letters, **2009**. 9(10): p. 3669-3670.

63. Korinek, P.M., *Amorphous fluoropolymers- a new generation of products.* Macromolecular Symposia, **1994**. 82: p. 61-65.

64. Zhang, H. and Weber, S.G., *Teflon af materials*, in *Fluorous chemistry*, I.T. Horvath, Editor. **2012**, Springer-Verlag Berlin: Berlin. p. 307-337.

65. Resnick, P.R. and Buck, W.H., *Teflon® af: A family of amorphous fluoropolymers with extraordinary properties*, in *Fluoropolymers 2*. **2002**, Springer. p. 25-33.

66. Czolkos, I., Guan, J., Orwar, O., and Jesorka, A., *Flow control of thermotropic lipid monolayers.* Soft Matter, **2011**. 7(15): p. 6926-6933.

67. Rustom, A., Saffrich, R., Markovic, I., Walther, P., and Gerdes, H.-H., *Nanotubular highways for intercellular organelle transport.* Science, **2004**. 303(5660): p. 1007-1010.

68. Karlsson, A., Karlsson, R., Karlsson, M., Cans, A.S., Stromberg, A., Ryttsen, F., and Orwar, O., *Molecular engineering - networks of nanotubes and containers.* Nature, **2001**. 409(6817): p. 150-152.

69. Jesorka, A., Stepanyants, N., Zhang, H.J., Ortmen, B., Hakonen, B., and Orwar, O., *Generation of phospholipid vesicle-nanotube networks and transport of molecules therein.* Nature Protocols, **2011**. 6(6): p. 791-805.

70. Derényi, I., Koster, G., Van Duijn, M.M., Czövek, A., Dogterom, M., and Prost, J., *Membrane nanotubes*, in *Controlled nanoscale motion*, H. Linke and A. Månsson, Editors. **2007**, Springer Berlin Heidelberg. p. 141-159.

71. Lobovkina, T., Dommersnes, P., Joanny, J.F., and Orwar, O., *Formation and release of circular lipid nanotubes.* Soft Matter, **2008**. 4(3): p. 467-470.

72. Castillo, J.A., Narciso, D.M., and Hayes, M.A., *Bionanotubule formation from surface-attached liposomes using electric fields.* Langmuir, **2009**. 25(1): p. 391-396.

73. Bi, H.M., Fu, D.G., Wang, L., and Han, X.J., *Lipid nanotube formation using space-regulated electric field above interdigitated electrodes.* Acs Nano, **2014**. 8(4): p. 3961-3969.

74. Frusawa, H., Manabe, T., Kagiyama, E., Hirano, K., Kameta, N., Masuda, M., and Shimizu, T., *Electric moulding of dispersed lipid nanotubes into a nanofluidic device.* Scientific Reports, **2013**. 3.

75. Jesorka, A., Stepanyants, N., Zhang, H., Ortmen, B., Hakonen, B., Orwar, O., Department of, C., Biological Engineering, N.C., Chalmers University of, T., Chalmers Tekniska, H., Institutionen För Kemi- Och Bioteknik, F.K., Institutionen För Kemi- Och Bioteknik, K., and Biological Engineering, P.C., *Generation of phospholipid vesicle-nanotube networks and transport of molecules therein.* Nature Protocols, **2011**. 6(6): p. 791-805.

76. Lizana, L., Bauer, B., and Orwar, O., *Controlling the rates of biochemical reactions and signaling networks by shape and volume changes.* Proceedings of the National Academy of Sciences of the United States of America, **2008**. 105(11): p. 4099-4104.

77. Derenyi, I., Julicher, F., and Prost, J., *Formation and interaction of membrane tubes.* Physical Review Letters, **2002**. 88(23).

78. Koster, G., Vanduijn, M., Hofs, B., and Dogterom, M., *Membrane tube formation from giant vesicles by dynamic association of motor proteins.* Proceedings of the National Academy of Sciences, **2003**. 100(26): p. 15583-15588.

79. Davis, D.M. and Sowinski, S., *Membrane nanotubes: Dynamic long-distance connections between animal cells.* Nature Reviews. Molecular Cell Biology, **2008**. 9(6): p. 431-6.

80. Cuvelier, D., Derényi, I., Bassereau, P., and Nassoy, P., *Coalescence of membrane tethers: Experiments, theory, and applications.* Biophysical Journal, **2005**. 88(4): p. 2714-2726.

81. Gozen, I. and Jesorka, A., *Instrumental methods to characterize molecular phospholipid films on solid supports.* Analytical Chemistry, **2012**. 84(2): p. 822-838.

82. Gözen, I., Billerit, C., Dommersnes, P., Jesorka, A., and Orwar, O., *Calcium-ion-controlled nanoparticle-induced tubulation in supported flat phospholipid vesicles.* Soft Matter, **2011**. 7(20): p. 9706-9713.

83. Reboiras, M., *Activity coefficients of cacl2 and mgcl2 in the presence of dipalmitoylphosphatidylcholine-phosphatidylinositol vesicles in aqueous media.* Bioelectrochemistry and Bioenergetics, **1996**. 39(1): p. 101-108.

84. Lobovkina, T., Gozen, I., Erkan, Y., Olofsson, J., Weber, S.G., and Orwar, O., *Protrusive growth and periodic contractile motion in surface-adhered vesicles induced by ca2+-gradients.* Soft Matter, **2010**. 6(2): p. 268-272.

85. Nissen, J., Gritsch, S., Wiegand, G., and Rädler, J.O., *Wetting of phospholipid membranes on hydrophilic surfaces - concepts towards self-healing membranes.* The European Physical Journal B, **1999**. 10(2): p. 335-344.

86. Radler, J., Strey, H., and Sackmann, E., *Phenomenology and kinetics of lipid bilayer spreading on hydrophilic surfaces.* Langmuir, **1995**. 11(11): p. 4539-4548.

87. Akashi, K.-I., Miyata, H., Itoh, H., and Kinosita, K., *Formation of giant liposomes promoted by divalent cations: Critical role of electrostatic repulsion.* Biophysical Journal, **1998**. 74(6): p. 2973-2982.

88. Resnick, P.R., *The preparation and properties of a new family of amorphous fluoropolymers - teflon-af*. Advanced electronic packaging materials, ed. A.T. Barfknecht, J.P. Partridge, C.J. Chen, and C.Y. Li. Vol. 167. **1990**, Pittsburgh: Materials Research Soc. 105-110.

89. Arcella, V., Ghielmi, A., and Tommasi, G., *High performance perfluoropolymer films and membranes.* Annals of the New York Academy of Sciences, **2003**. 984(1): p. 226-244.

90. Resnik, P.R.B., W. H., *Teflon®af: A family of amorphous fluoropolymers with extraordinary properties*, in *Fluoropolymers 2: Properties*, G. Hougham, P.E. Cassidy, K. Johns, and T. Davidson, Editors. **2002**, Springer US: Boston, MA.

91. Ebnesajjad, S. and Sciencedirect, *Introduction to fluoropolymers: Materials, technology and applications*. **2013**, San Diego: Elsevier Science & Technology Books.

92. Yang, M.K., French, R.H., and Tokarsky, E.W., *Optical properties of teflon® af amorphous fluoropolymers.* Journal of Micro/Nanolithography, MEMS, and MOEMS, **2008**. 7(3).

93. Tokarev, A.V., Bondarenko, G.N., and Yampol'skii, Y.P., *Chain structure and stiffness of teflon af glassy amorphous fluoropolymers.* Polymer Science Series A, **2007**. 49(8): p. 909-920.

94. Voraberger, H.S., Trettnak, W., and Ribitsch, V., *Optochemical hydrogen peroxide sensor based on oxygen detection.* Sensors & Actuators: B.Chemical, **2003**. 90(1): p. 324-331.

95. Hughes, L.D. and Devol, T.A., *Characterization of a teflon® coated semiconductor detector flow cell for monitoring of pertechnetate in groundwater.* Journal of Radioanalytical and Nuclear Chemistry, **2006**. 267(2): p. 287-295.

96. Harwood, J. and Ieee, *Teflon af- a new polymer for electronics.* 8th Iemt 1990 : International Electronic Manufacturing Technology Symposium, **1990**: p. 503-507.

97. Gunther, P., Ding, H., Gerhardmulthaupt, R., and Ieee, *Electret properties of spin-coated teflon-af films.* Ieee 1993 annual report: Conference on electrical insulation and dielectric phenomena. **1993**, New York: I E E E. 197-202.

98. Lu, T.J., *Charge storage in teflon af films.* Ise 9 - 9th international symposium on electrets, proceedings, ed. Z.F. Xia and H.Y. Zhang. **1996**, New York: I E E E. 66-71.

99. Teng, H.X., *Overview of the development of the fluoropolymer industry.* APPLIED SCIENCES-BASEL, **2012**. 2(2): p. 496-512.

100. Rego, R., Caetano, N.D., and Mendes, A., *Development of a new gas sensor for binary mixtures based on the permselectivity of polymeric membranes.* Analytica Chimica Acta, **2004**. 511(2): p. 215-221.

101. Rego, R., Caetano, N., and Mendes, A., *Hydrogen/methane and hydrogen/nitrogen sensor based on the permselectivity of polymeric membranes.* Sensors & Actuators: B.Chemical, **2005**. 111(Complete): p. 150-159.

102. O'brien, M., Baxendale, I.R., and Ley, S.V., *Flow ozonolysis using a semipermeable teflon af-2400 membrane to effect gas - liquid contact.* Organic letters, **2010**. 12(7): p. 1596-1598.

103. Thomas, P.C., Halter, M., Tona, A., Raghavan, S.R., Plant, A.L., and Forry, S.P., *A noninvasive thin film sensor for monitoring oxygen tension during in vitro cell culture.* Analytical Chemistry, **2009**. 81(22): p. 9239-9246.

104. Du, W.-B., Fang, Q., He, Q.-H., and Fang, Z.-L., *High-throughput nanoliter sample introduction microfluidic chip-based flow injection analysis system with gravity-driven flows.* Analytical Chemistry, **2005**. 77(5): p. 1330-1337.

105. Anamelechi, C.C., Truskey, G.A., and Reichert, W.M., *Mylar™ and teflon-af™ as cell culture substrates for studying endothelial cell adhesion.* Biomaterials, **2005**. 26(34): p. 6887-6896.

106. Valle, F., Chelli, B., Bianchi, M., Greco, P., Bystrenova, E., Tonazzini, I., and Biscarini, F., *Stable non-covalent large area patterning of inert teflon-af surface: A new approach to multiscale cell guidance.* Advanced Engineering Materials, **2010**. 12(6): p. B185-B191.

107. Makohliso, S.A., Giovangrandi, L., Leonard, D., Mathieu, H.J., Ilegems, M., and Aebischer, P., *Application of teflon-af (r) thin films for bio-patterning of neural cell adhesion.* Biosensors & Bioelectronics, **1998**. 13(11): p. 1227-1235.

108. Kuo, C.W., Shiu, J.-Y., Whang, W.-T., and Chen, P., *Addressable cell microarrays via switchable superhydrophobic surfaces.* Journal of Adhesion Science and Technology, **2010**. 24(5): p. 1023-1030.

109. Shaali, M., Lara-Avila, S., Dommersnes, P., Ainla, A., Kubatkin, S., and Jesorka, A., *Nanopatterning of mobile lipid mono layers on electron-beam-sculpted teflon af surfaces.* Acs Nano, **2015**. 9(2): p. 1271-1279.

110. Costela, A., Garciamoreno, I., Florido, F., Figuera, J.M., Sastre, R., Hooker, S.M., Cashmore, J.S., and Webb, C.E., *Laser-ablation of polymeric materials at 157 nm.* Journal of Applied Physics, **1995**. 77(6): p. 2343-2350.

111. Miyoshi, N., Oshima, A., Urakawa, T., Fukutake, N., Nagai, H., Gowa, T., Takasawa, Y., Takahashi, T., Numata, Y., Katoh, T., Katoh, E., Tagawa, S., and Washio, M., *Nano- and micro-fabrication of perfluorinated polymers using quantum beam technology.* Radiation Physics and Chemistry, **2011**. 80(2): p. 230-235.

112. Fukutake, N., Miyoshi, N., Takasawa, Y., Urakawa, T., Gowa, T., Okamoto, K., Oshima, A., Tagawa, S., and Washio, M., *Micro- and nano-scale fabrication of fluorinated polymers by direct etching using focused ion beam.* Japanese Journal of Applied Physics, **2010**. 49(6).

113. Katoh, T., Nishi, N., Fukagawa, M., Ueno, H., and Sugiyama, S., *Direct writing for three-dimensional microfabrication using synchrotron radiation etching.* Sensors and Actuators a-Physical, **2001**. 89(1-2): p. 10-15.

114. Kobayashi, A., Oshima, A., Okubo, S., Tsubokura, H., Takahashi, T., Oyama, T.G., Tagawa, S., and Washio, M., *Thermal and radiation process for nano-/micro-fabrication of crosslinked ptfe.* Nuclear Instruments & Methods in Physics Research Section B-Beam Interactions with Materials and Atoms, **2013**. 295: p. 76-80.

115. Mayer, M., Kriebel, J.K., Tosteson, M.T., and Whitesides, G.M., *Microfabricated teflon membranes for low-noise recordings of ion channels in planar lipid bilayers.* Biophysical Journal, **2003**. 85(4): p. 2684-2695.

116. Karre, V., Keathley, P.D., Guo, J., and Hastings, J.T., *Direct electron-beam patterning of teflon af.* Ieee Transactions on Nanotechnology, **2009**. 8(2): p. 139-141.

117. Zhao, H., Ismail, K., and Weber, S.G., *How fluorous is poly(2,2-bis(trifluoromethyl)-4,5-difluoro-1,3-dioxide-co-tetrafluoroeth ylene) (teflon af)?* Journal of the American Chemical Society, **2004**. 126(41): p. 13184-13185.

118. Lai, C.Z., Koseoglu, S.S., Lugert, E.C., Boswell, P.G., Rabai, J., Lodge, T.P., and Buhlmann, P., *Fluorous polymeric membranes for ionophore-based ion-selective potentiometry: How inert is teflon af?* Journal of the American Chemical Society, **2009**. 131(4): p. 1598-1606.

119. Lu, T. *Charge storage in teflon af films*.

120. Popovici, D., Sacher, E., and Meunier, M., *Photodegradation of teflon af1600 during xps analysis.* Journal of Applied Polymer Science, **1998**. 70(6): p. 1201-1207.

121. Forsythe, J.S., Hill, D.J.T., Logothetis, A.L., and Whittaker, A.K., *The radiation chemistry of the copolymer of tetrafluoroethylene with 2,2-bis(trifluoromethyl)-4,5-difluoro-1,3-dioxole.* Polymer Degradation and Stability, **1999**. 63(1): p. 95-101.

122. Van Delft, F.C.M.J.M., Weterings, J.P., Van Langen-Suurling, A.K., and Romijn, H., *Hydrogen silsesquioxane/novolak bilayer resist for high aspect ratio nanoscale electron-beam lithography.* Journal of Vacuum Science&Technology B: Microelectronics and Nanometer Structures, **2000**. 26(6): p. 3419-3423.

123. Grigorescu, A.E. and Hagen, C.W., *Resists for sub-20-nm electron beam lithography with a focus on hsq: State of the art.* Nanotechnology, **2009**. 20(29): p. 292001.

124. Adams, T.M. and Layton, R.A., *Introductory mems: Fabrication and applications*. Vol. 1. **2010**, New York: Springer. 1-444.

125. Conradie, E.H. and Moore, D.F., *Su-8 thick photoresist processing as a functional material for mems applications.* Journal of Micromechanics and Microengineering, **2002**. 12(4): p. 368-374.

126. Pease, R.F.W., *Electron - beam lithography* Contemporary Physics, **1981**. 22(3): p. 265-290.

127. Thornley, R.F.M. and Sun, T., *Electron beam exposure of photoresists.* Journal of the Electrochemical Society, **1965**. 112(11): p. 1151.

128. Chang, T.H.P., *Proximity effect in electron-beam lithography* Journal of Vacuum Science & Technology, **1975**. 12(6): p. 1271-1275.

129. Helbert, J.N. and Sciencedirect, *Handbook of vlsi microlithography: Principles, technology, and applications*. **2001**, Norwich, N.Y; Park Ridge, N.J: Noyes Publications.

130. Zhou, Z.J., *Electron beam lithography*, in *Handbook of microscopy for nanotechnology*, Z.L.W. Nan Yao, Editor. **2005**, Springer US: New York. p. pp 287-321.

131. Ford, B.J., *The earliest views.* Scientific American, **1998**. 278(4): p. 50-53.

132. Ishikawa-Ankerhold, H.C., Ankerhold, R., and Drummen, G.P.C., *Advanced fluorescence microscopy techniques-frap, flip, flap, fret and flim.* Molecules, **2012**. 17(4): p. 4047-4132.

133. Stephens, D.J. and Allan, V.J., *Light microscopy techniques for live cell imaging.* Science, **2003**. 300(5616): p. 82-86.

134. Allen, R.D., David, G.B., and Nomarski, G., *The zeiss nomarski differential interference equipment for transmitted light microscopy.* Mikrosk.Mikrosk.Tech, **1969**. 69(4): p. 193-221.

135. Albani, J.R. and Ebrary, *Principles and applications of fluorescence spectroscopy*. Vol. 1. **2007**, Oxford; Ames, Iowa: Blackwell Science. 1-255.

136. Rust, M.J., Bates, M., and Zhuang, X.W., *Sub-diffraction-limit imaging by stochastic optical reconstruction microscopy (storm).* Nature Methods, **2006**. 3(10): p. 793-795.

137. Chozinski, T.J., Gagnon, L.A., and Vaughan, J.C., *Twinkle, twinkle little star: Photoswitchable fluorophores for super-resolution imaging.* Febs Letters, **2014**. 588(19): p. 3603-3612.

138. Lang, H.P. and Gerber, C., *How the doors to the nanoworld were opened.* Nature Nanotechnology, **2006**. 1(1): p. 3-5.

139. Rugar, D. and Hansma, P., *Atomic force microscopy*. Physics Today, **1990**. 43(10): p. 23.

140. Tsukruk, V.V., Singamaneni, S., and Ebrary, *Scanning probe microscopy of soft matter*. **2011**, Hoboken: Wiley-VCH [Imprint].

141. Raman, A., Trigueros, S., Cartagena, A., Stevenson, A.P.Z., Susilo, M., Nauman, E., and Contera, S.A., *Mapping nanomechanical properties of live cells using multi-harmonic atomic force microscopy.* Nature Nanotechnology, **2011**. 6(12): p. 809-814.

142. Hartmann, U., *Magnetic force microscopy*. Annual Review of Materials Science, **1999**. 29(1): p. 53-87.

143. Melitz, W., Shen, J., Kummel, A.C., and Lee, S., *Kelvin probe force microscopy and its application.* Surface Science Reports, **2011**. 66(1): p. 1-27.

144. Nonnenmacher, M., Oboyle, M.P., and Wickramasinghe, H.K., *Kelvin probe force microscopy.* Applied Physics Letters, **1991**. 75(25): p. 2921-2923.

145. Jacobs, H.O., Knapp, H.F., and Stemmer, A., *Practical aspects of kelvin probe force microscopy.* Review of Scientific Instruments, **1999**. 79(3): p. 1756-1760.

146. Everhart, T.E. and Thornley, R.F.M., *Wide-band detector for micro-microampere low-energy electron currents.* Journal of scientific instruments, **1960**. 37(7): p. 246-248.

147. Michler, G.H. and Springerlink, *Electron microscopy of polymers*. Vol. 1. Aufl. **2008**, Berlin: Springer.

148. Newbury, D.E. and Ritchie, N.W.M., *Performing elemental microanalysis with high accuracy and high precision by scanning electron microscopy/silicon drift detector energy-dispersive x-ray spectrometry (sem/sdd-eds).* Journal of Materials Science, **2015**. 50(2): p. 493-518.

149. Watson, J.D. and Crick, F.H.C., *Molecular structure of nucleic acids - a structure for deoxyribose nueleic acid.* Nature, **1953**. 171(4356): p. 737-738.

150. Tan, S.J., Campolongo, M.J., Luo, D., and Cheng, W.L., *Building plasmonic nanostructures with DNA.* Nature Nanotechnology, **2011**. 6(5): p. 268-276.

151. Bhatia, D., Surana, S., Chakraborty, S., Koushika, S.P., and Krishnan, Y., *A synthetic icosahedral DNA-based host-cargo complex for functional in vivo imaging.* Nature Communications, **2011**. 2.

152. Bath, J. and Turberfield, A.J., *DNA nanomachines.* Nature Nanotechnology, **2007**. 2(5): p. 275-284.

153. Elbaz, J., Lioubashevski, O., Wang, F.A., Remacle, F., Levine, R.D., and Willner, I., *DNA computing circuits using libraries of dnazyme subunits.* Nature Nanotechnology, **2010**. 5(6): p. 417-422.

154. *The unnatural order of things.* Nature Nanotechnology, **2009**. 4(4): p. 203-203.

155. Rothemund, P.W.K., *Folding DNA to create nanoscale shapes and patterns.* Nature, **2006**. 440(7082): p. 297-302.

156. Roh, Y.H., Ruiz, R.C.H., Peng, S.M., Lee, J.B., and Luo, D., *Engineering DNA-based functional materials.* Chemical Society Reviews, **2011**. 40(12): p. 5730-5744.

157. Jungmann, R., Steinhauer, C., Scheible, M., Kuzyk, A., Tinnefeld, P., and Simmel, F.C., *Single-molecule kinetics and super-resolution microscopy by fluorescence imaging of transient binding on DNA origami.* Nano Letters, **2010**. 10(11): p. 4756-4761.

158. Dutta, P.K., Varghese, R., Nangreave, J., Lin, S., Yan, H., and Liu, Y., *DNA-directed artificial light-harvesting antenna.* Journal of the American Chemical Society, **2011**. 133(31): p. 11985-11993.

159. Kjems, J., Tørring, T., Jacobsen, M.F., Subramani, R., Rotaru, A., Mokhir, A., Mamdouh, W., Gothelf, K.V., Ravnsbæk, J.B., Besenbacher, F., and Voigt, N.V., *Single-molecule chemical reactions on DNA origami.* Nature Nanotechnology, **2010**. 5(3): p. 200-203.

160. Davis, J. and Ebrary, *Animal cell culture: Essential methods.* Vol. 1. Aufl.; 1. **2011**, Hoboken, NJ: John Wiley & Sons Inc.